Manufacturers of perchlorate-containing products and those using perchlorate in operations

Table 1 shows some of the perchlorate-containing products and the purpose of perchlorate use in manufacturing processes. Manufacturers of perchlorate-containing products and manufacturers using perchlorate in operations are considered to be potential sources of perchlorate in the environment.

In the United States, manufacturing of propellants, explosives, ordnance, rockets, and flares was included as potential source of perchlorate release into the environment as of April 2003 by the US EPA. Among the data on the list for which the suspected source was a manufacturer of perchlorate-containing products, the highest perchlorate concentration was 640 000 $\mu g\,l^{-1}$ observed in monitoring of well waters in Arkansas and California, and both the suspected sources were rocket manufacturers. In Japan, perchlorate was detected at 400 $\mu g\,l^{-1}$ in a river in Okayama prefecture, and a chemical facility manufacturing airbags located upstream was the likely source of contamination. However, perchlorate was present at levels ranging from below the limit of detection to 3.26 $\mu g\,l^{-1}$ in a public water system (PWS) of the Town of Tewksbury, Massachusetts, its source being the Merrimack River. The source of perchlorate in the river was industrial effluent from a perchloric acid user.

Usage of perchlorate-containing products

As shown in **Table 1**, perchlorate compounds are used in various products and their use may result in perchlorate contamination in the environment. Solid propellants and munitions are the main applications of perchlorate compounds in the United States. However, commercial explosives and fireworks are also known to be potential sources of perchlorate.

Solid propellants

Among the perchlorate compounds, ammonium perchlorate is commonly used in solid rocket/missile propellants. Launch failure and the disposal of solid propellants may result in the release of perchlorate into the environment. Manufacturing, testing, research, handling, and disposal of rockets and propellants were included as potential sources of perchlorate release into the environment as of April 2003 by the US EPA. The facilities of propellant users, for example, the Department of Defense (DOD) and the National Aeronautics and Space Administration (NASA), are also listed under known sources of perchlorate release in the United States as of March 2005. High levels of perchlorate, at levels of thousands or tens of thousands of micrograms per liter, were detected at some of these sites.

Munitions

Perchlorate may be contained in munitions, munition components, and training devices, including solid fuel rockets, mines, torpedo warheads, smoke-generating compounds, signal flares, parachute flares, star rounds for pistols (illumination rounds), thermite-type incendiaries, tracer rounds, incendiary bombs, fuses, jet-assisted take-off devices, and training simulators. Perchlorate contamination may occur through their storage, disposal, or use. Perchlorate contamination has been reported at many military facilities in the United States. Sixty-three DOD facilities in 25 states were listed by the US EPA as known perchlorate releasers in the United States as of March 2005. Perchlorate contamination in drinking water, groundwater, or surface water was reported in 54 of these 63 facilities (**Table 2**). The highest perchlorate concentrations detected were 720 $\mu g\,l^{-1}$ in drinking water, 276 000 $\mu g\,l^{-1}$ in groundwater, and 16 000 $\mu g\,l^{-1}$ in surface water.

Commercial explosives

Perchlorate salts, such as sodium, ammonium, and potassium perchlorate, are used in some explosive products. They are used as emulsions, water gels, delay elements in detonators, and in some seismic explosives. Perchlorate contamination may occur through the incomplete detonation of these products.

The sources of perchlorate contamination in three PWSs in the towns of Millbury, Westford, and Boxborough, Massachusetts, are suspected to have resulted from the explosives used at construction sites. In Millbury, perchlorate was detected from two PWSs wells at concentrations of 45.3 and 21.6 $\mu g\,l^{-1}$, respectively, in May 2004. Perchlorate was also detected in surface water runoff systems and monitoring wells at levels ranging from tens to hundreds of micrograms per liter. Explosives

Table 1 Some perchlorate-containing products and manufacturing processes using perchlorate compounds (ITRC perchlorate team and MA DEP)

Use of perchlorate compound		
Additive in polyvinyl chloride	Engine oil testing	Paints and enamels
Airbag initiators	Etching of brass and copper	Photographic flash powder
Analytical testing agents	Explosives	Propellant in rocket engines
Ejection seats	Fireworks	Road flares
Electroplating operations	Leather tanning	Safety matches
Electropolishing operations	Oxygen generators	Textile bleaching agent

Table 2 Known perchlorate contamination in drinking water, groundwater, and surface water at DOD facilities as of March 2005

Category	*No. of facilities*	*No. of states*	*Highest perchlorate detection*		
			Concentration ($\mu g\,l^{-1}$)	*Facility/site*	*State*
Drinking water	11	6	720	China Lake	California
Groundwater	44	22	276 000	Naval Surface Warfare Center, Indian Head Division	Maryland
Surface water	16	8	16 000	Holloman Air Force Base	New Mexico

Note: The lists do not show the entire detection of perchlorate in drinking water, groundwater, and surface water at DOD facilities. They represent the extent of perchlorate detection data currently known to the US EPA as reported from various sources. Perchlorate was detected in some categories (drinking water, groundwater, and surface water) at the same facilities. The total number of DOD facilities and states where perchlorate was detected were 54 and 24, respectively. In some cases, only the fact that perchlorate was detected was reported.

containing perchlorate that were used at the construction site are suspected to have been the source of the perchlorate. In Westford, perchlorate was found at $2\,\mu g\,l^{-1}$ from a PWSs well in July 2004. By subsequent investigation, MA DEP concluded that blasting at the highway garage site using explosives containing up to 30% ammonium perchlorate was the likely source of perchlorate. In Boxborough, perchlorate was detected in two of five condominium wells, with a peak concentration of $1300\,\mu g\,l^{-1}$. MA DEP suspected blasting at a construction site of a new wastewater treatment plant to be the source of perchlorate, although information about the types of explosives used was not obtained.

Fireworks

Fireworks are a potential source of perchlorate contamination due to atmospheric deposition and debris. MA DEP reported that fireworks displays were likely sources of perchlorate contamination ($\geq 1\,\mu g\,l^{-1}$) for at least three PWSs. These three PWSs are small, noncommunity wells, and the perchlorate concentrations in the wells were primarily of the order of micrograms per liter. The effects of fireworks displays on perchlorate concentration in a small lake located in Ada, Oklahoma, were also investigated from 2004 to 2006. Perchlorate concentrations preceding fireworks displays in the lake ranged from 0.005 to $0.081\,\mu g\,l^{-1}$, with a mean value of $0.043\,\mu g\,l^{-1}$, and increased within 14 hours after each of the displays. The maximum perchlorate concentration observed after the display in July 2006 was $44.2\,\mu g\,l^{-1}$. Since then, perchlorate concentrations decreased and returned to the background level within 20–80 days after the display. In addition, it was reported that the perchlorate concentration of a river in Japan was affected by a fireworks display, rising to a high concentration of $79\,\mu g\,l^{-1}$ just after the display conducted on a barge on the river. As the perchlorate concentration at the same location dropped to $0.39\,\mu g\,l^{-1}$ 5 days after the display, fireworks displays are considered to have short-term effects on perchlorate concentration in the river.

A field study of the impact of fireworks displays on perchlorate contamination was conducted on the University of Massachusetts campus by MA DEP. Fireworks displays had occurred at the site since 1995, and eight monitoring wells installed at the location allowed sampling to take place from June 2004, before the annual fireworks display, to July 2006. Perchlorate concentration in groundwater ranged from not detected to $62.2\,\mu g\,l^{-1}$ in the 2004 predisplay sample, where the groundwater showed contamination from earlier fireworks displays. It was also indicated that the impact of perchlorate on groundwater from the launch area may be migrating downgradient.

Unintended by-product

Sodium perchlorate is manufactured electrolytically from sodium chlorate, which is manufactured from brine in the electrolysis process. Manufacture of sodium chlorate is a potential source of perchlorate because perchlorate is generated as an unintended by-product in the electrolysis process. Sodium chlorate is used as herbicide, mainly as a defoliant. It was reported that perchlorate content in one chlorate defoliant was $24\,mg\,kg^{-1}$. It was also reported that perchlorate is generated as an unintended by-product in electrolysis processes other than those for the manufacture of perchlorate and chlorate.

Perchlorate contamination in the Tone River Basin, Japan, was discovered in 2006 (**Figure 1**). As mentioned earlier, two industrial effluents were the main sources of perchlorate: one from a facility manufacturing perchlorate and chlorate and the other from a facility conducting electrolysis processes other than those for the manufacture of perchlorate and chlorate. In the latter case, the perchlorate concentration in the industrial effluent was $15\,000\,\mu g\,l^{-1}$, and it was concluded that perchlorate was generated as an unintended by-product of

the electrolysis processes. The effluent entered the Usui River, one of the tributaries of the Tone River, and the maximum concentration of perchlorate in the Usui River was 2300 $\mu g\,l^{-1}$. The estimated perchlorate load from the industrial effluent was 40–78 kg per day, which was comparable to that from the manufacture of perchlorate and chlorate located near the Tone River.

Perchlorate as an unintended by-product was also reported in a water distribution system. In 2002, perchlorate concentration was determined by the Texas Commission for Environmental Quality to be 32 $\mu g\,l^{-1}$ in an elevated storage tank. A subsequent investigation concluded that the most likely source of perchlorate was the storage tank itself, where perchlorate was generated electrochemically *in situ* from chlorinated drinking water in the corrosion protection system. Laboratory experiments confirmed this suspicion. It was also suggested that perchlorate generation was dependent on the type of metal used for the anode.

Hypochlorite solution, which is used as a disinfectant in water purification processes, is known to contain perchlorate alongside other oxihalides (e.g., chlorite, chlorate, and bromate) as impurities. Hypochlorite solutions used in water systems (PWSs or private water systems) are typically commercial sodium hypochlorite solutions or on-site hypochlorite solutions generated by the electrolysis of brine. It was reported that perchlorate concentrations in 32 commercial hypochlorite solutions and 6 hypochlorite solutions generated on-site that were used in water systems were in the range of 170–33 000 $\mu g\,l^{-1}$ (median concentration, 2300 $\mu g\,l^{-1}$) and 13–660 $\mu g\,l^{-1}$ (median concentration, 32 $\mu g\,l^{-1}$), respectively (**Table 3**). Perchlorate concentrations in the hypochlorite solutions were higher in cases in which the levels of free available chlorines (FACs) in the solutions measured in the laboratory (8.0–16.4%) were lower. Perchlorate concentrations in the commercial hypochlorite solutions are considered to increase in accordance with the decay of FACs in the solutions. Another study showed that perchlorate concentrations in hypochlorite solutions increase during storage. In general, the concentration of perchlorate originating from hypochlorite solution is low in finished drinking water (0.2–0.4 $\mu g\,l^{-1}$). However, in two cases in Japan, the perchlorate concentration in finished drinking water in a PWS was found to be $\geq 1\,\mu g\,l^{-1}$ (6.1 $\mu g\,l^{-1}$ in October 2006 and 1.1 $\mu g\,l^{-1}$ in February 2007). The hypochlorite disinfectant was the suspected source in both cases as perchlorate concentrations in the raw waters were low ($<0.05\,\mu g\,l^{-1}$) and those in the hypochlorite solutions were high (13 000 $\mu g\,l^{-1}$ in February 2007). Such cases highlight the risks of perchlorate contamination in water systems by hypochlorite solutions with low FACs and perchlorate accumulation.

Occurrence of Perchlorate in Drinking Water

Since the discovery of perchlorate in drinking water wells in eastern Sacramento County, California, in 1997 by CA DHS, the occurrence of perchlorate in water systems has been investigated throughout the United States. In the case of Japan, the occurrence of perchlorate in drinking water sources and some tap waters was first reported in 2006, and studies of its occurrence in water systems, including a national survey, were subsequently conducted. Despite a limited number of investigations of the occurrence of perchlorate, perchlorate contamination of water systems in some other countries has been reported. It is difficult to remove perchlorate in the conventional water purification processes and ozone/activated carbon processes because perchlorate is highly soluble in water. Ion exchange and anaerobic biological treatment processes are techniques available for such processing. Perchlorate concentrations in various types of bottled water (e.g., drinking waters of PWSs, spring waters, and well waters) of various countries have also been investigated.

Drinking Water in Water Systems

United States

A national survey of perchlorate in PWSs was conducted in 2001–05 under the first Unregulated Contaminant Monitoring Regulation (UCMR 1). The UCMR program collects data on contaminants suspected to be present in drinking water but that do not have health-based

Table 3 Perchlorate concentration in hypochlorite solution used in water systems

Category	*No. of samples detected/no. of samples analyzed*	*Range of FAC measured (%)*	*Perchlorate concentration ($\mu g\,l^{-1}$)*	
			Range	*Median*
Commercial hypochlorite solution	32/32	8.0–16.4	170–33 000	2300
On-site generation	6/6	1.0–7.2	13–660	32

Note: Samples were collected in September–October 2006, except for five commercial hypochlorite solutions that were collected in February–March 2007. The range of labeled FACs in commercial hypochlorite solutions was 12–13.2%, except in four samples for which data could not be obtained.

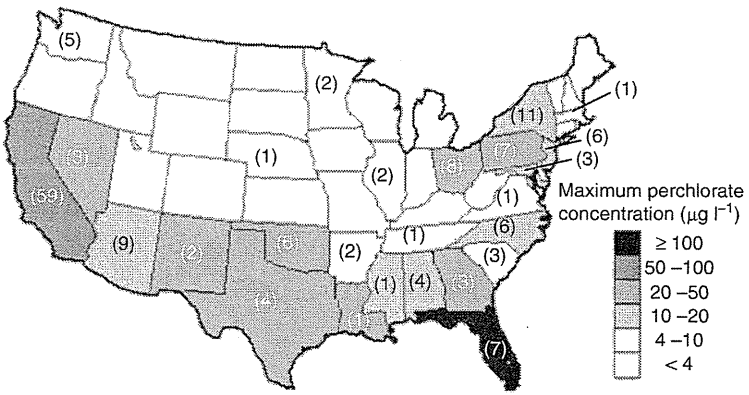

Figure 2 Maximum perchlorate concentrations in PWSs by UCMR 1 (final data set). The detection data are available from the website of US EPA. Numbers in parentheses are the number of PWSs in each state or territory in which perchlorate was detected at $\geq 4\,\mu g\,l^{-1}$. Alaska and Hawaii are not illustrated but perchlorate was not detected in these states.

standards set under the Safe Drinking Water Act (SDWA). The results of perchlorate detection in UCMR 1 are shown in **Figure 2**. Perchlorate was found at a minimum reporting level (MRL) of $4\,\mu g\,l^{-1}$ or more in 160 of 3870 PWSs in 26 states and 2 territories, and in 647 of the 34 728 samples tested. The perchlorate concentrations detected were in the range of 4–420 $\mu g\,l^{-1}$, with a mean of $9.9\,\mu g\,l^{-1}$. The maximum perchlorate concentration, $420\,\mu g\,l^{-1}$, was found in a PWS in Puerto Rico. Of the 160 PWSs in which perchlorate was detected, 8 were small systems (supplying a population of $\leq 10\,000$) and 152 were large systems (supplying a population of $> 10\,000$). The contaminated water type was surface water in 3 of the 8 small systems and groundwater in the remaining 5, whereas for large systems, it was surface water for 88 of 152 and groundwater in the remaining 64. The US EPA occurrence data for UCMR 1 (the final data set) have been released and detailed analyses as of July 2005 are also available.

Statewide investigations of perchlorate in PWSs have also been conducted by several states in the United States (e.g., California, Massachusetts, Texas, and Arizona). In California, the occurrence of perchlorate in drinking water sources has been investigated by CA DHS since 1997. In 1999, perchlorate was added to the list of unregulated chemicals for which monitoring is required by CA DHS. According to the results from July 2003 to July 2008, perchlorate was detected at $\geq 4\,\mu g\,l^{-1}$ in 274 of approximately 10 600 sources. These 274 sources are active and standby sources of 82 PWSs in 12 counties and are mostly groundwater. The highest perchlorate concentrations in source water in each county ranged from 4 to $96\,\mu g\,l^{-1}$.

In Massachusetts, the statewide occurrence of perchlorate in community and nontransient/noncommunity PWSs was reported in 2005 and perchlorate was detected at $\geq 1\,\mu g\,l^{-1}$ in 9 of 591 PWSs investigated. The water type of eight of the nine PWSs was groundwater. The likely sources of perchlorate identified were blasting agents, fireworks, and industrial use of perchloric acid. According to perchlorate monitoring results as of March 2006, perchlorate was detected at $\geq 1\,\mu g\,l^{-1}$ from 10 PWSs. The highest perchlorate concentrations in finished drinking water in each PWS ranged from 1.51 to $1300\,\mu g\,l^{-1}$.

Japan

Perchlorate concentrations in a total of 66 water systems (46 PWSs and 20 private water systems) selected from across Japan were investigated in October 2006 and February 2007. In the survey of October 2006, perchlorate concentrations in tap waters of 3 of 41 water systems (21 PWSs and 20 private water systems) were $\geq 1\,\mu g\,l^{-1}$ (1.2–6.1 $\mu g\,l^{-1}$), which was confirmed by an additional survey conducted for these 3 water systems in March 2006 (1.1–1.7 $\mu g\,l^{-1}$). The sources of perchlorate in two of these three water systems were uncertain, with hypochlorite solution used for disinfection being the suspected source in the remaining water system. In the survey of February 2007, perchlorate concentrations in the tap waters of 4 of 25 PWSs were $\geq 1\,\mu g\,l^{-1}$ (5.5–15 $\mu g\,l^{-1}$). The source waters used for the four PWSs were river waters from the Tone River Basin. Another study reported perchlorate concentrations ranging from 0.06 to $37\,\mu g\,l^{-1}$ in 30 tap waters tested in February to June 2006. Perchlorate was found at levels of $\geq 1\,\mu g\,l^{-1}$ in tap waters from the Tone River Basin and perchlorate concentrations were $\geq 10\,\mu g\,l^{-1}$ in 13 tap waters examined. At present, in Japan, the area where drinking water is most widely contaminated by perchlorate is in the Tone River Basin.

Table 4 Perchlorate concentration in finished drinking water of 42 PWSs in the Tone River Basin, Japan, September–October 2006

Category	*Water type*	*No. of samples detected/no. of samples analyzed*[a,b]	*No. of PWSs detected/no. of PWSs investigated*[a,b]	*Range of perchlorate concentration* ($\mu g\,l^{-1}$)[c]
Upper basin	Surface water	0/6	0/6	0.12–0.86
	Groundwater	2/5	2/5	0.08–24
Middle basin	Surface water	21/22	15/16	0.22–14
Lower basin	Surface water	11/17	10/15	0.23–1.8

[a]The number of samples is higher than that of PWSs because several samples were collected from some PWSs.
[b]Detected level of perchlorate in finished drinking water is $\geq 1\,\mu g\,l^{-1}$.
[c]Perchlorate was detected at $\geq 0.05\,\mu g\,l^{-1}$ in all finished drinking waters.

In fact, a study on the occurrence of perchlorate in PWSs has focused on the Tone River Basin. Perchlorate concentrations in 42 PWSs in the Tone River Basin were investigated in September–October 2006 (Table 4). The numbers of PWSs in the upper, middle, and lower Tone River Basin found to have perchlorate concentrations $\geq 1\,\mu g\,l^{-1}$ in finished drinking waters were 2, 15, and 10, respectively. Widespread perchlorate contamination of drinking water in the Tone River Basin was demonstrated, although the perchlorate concentrations decrease in downstream areas.

Other Countries

In Korea, perchlorate concentrations in tap waters of four cities (Pusan, Daegu, Milyang, and Yangsan) were investigated in 2006. The source waters for drinking water supply of these four cities are the surface waters of the Nakdong River Basin. Perchlorate was detected from all seven tap waters sampled, in the range of 0.15–35 $\mu g\,l^{-1}$. Perchlorate was also detected in the range of <0.05 to $60\,\mu g\,l^{-1}$ in the Nakdong River and its tributaries. Perchlorate concentrations in the Yeongsan River, which is also used as the source of drinking water supply, were in the range of 0.08–2.5 $\mu g\,l^{-1}$, although the perchlorate concentrations in tap waters sourced from the Yeongsan River were not reported.

In China, perchlorate concentrations in PWSs in Beijing were investigated from September 2001 to July 2002. Perchlorate concentrations detected in finished drinking waters ranged from 0.2 to 6.8 $\mu g\,l^{-1}$. Perchlorate contamination was observed in the finished drinking water drawn from raw groundwater. Examination of seasonal variations of perchlorate concentration in finished drinking water revealed the highest concentration in November, the drought season.

In Canada, it was reported that perchlorate concentrations in 12 tap waters of 12 cities in 3 provinces ranged from 0.016 to $0.168 \pm 0.004\,\mu g\,l^{-1}$. For five of these tap waters, the effects of filtration using either a household water filter or the reverse osmosis system on perchlorate concentrations in tap waters were investigated, and decrease in the perchlorate concentrations in all tap waters was reported (perchlorate concentrations in tap waters before filtration, 0.035 ± 0.001 to $0.089 \pm 0.001\,\mu g\,l^{-1}$; after filtration, 0.005 to $0.012 \pm 0.001\,\mu g\,l^{-1}$).

Bottled Water

In the fiscal year (FY) 2004 (i.e., from 1 October 2003 to 30 September, 2004), the US Food and Drug Administration (FDA) investigated perchlorate concentrations in bottled waters (e.g., drinking waters from PWSs and spring waters) collected from across the United States and found that perchlorate concentrations in 50 of 51 bottled waters were $<0.5\,\mu g\,l^{-1}$ and that in the remaining one bottled water was $0.56\,\mu g\,l^{-1}$. It was also reported that perchlorate concentrations in 21 bottled waters purchased from various local merchants representing various source types (e.g., drinking waters from PWSs, spring waters, and artesian waters) and treatment processes ranged from <0.05 to $0.74\,\mu g\,l^{-1}$. In 2004, the Massachusetts DPH reported that perchlorate concentrations in 50 bottled waters (e.g., drinking waters from PWS, spring waters, and artesian well waters) of 6 countries (i.e., United States, Canada, France, Italy, Norway, and Fiji) for sale in Massachusetts, which were submitted by bottled water companies, were $<1\,\mu g\,l^{-1}$. Of the data submitted by the bottled water companies, some were perchlorate concentrations in finished bottled water and others were those in source waters. It was also reported that perchlorate concentrations in 9 of 10 bottled waters from 5 countries (i.e., France, India, Germany, Canada, and Portugal) were low, ranging from below the level of detection to $0.198 \pm 0.017\,\mu g\,l^{-1}$, and that in the remaining 1 bottled water from Portugal was $5.098 \pm 0.040\,\mu g\,l^{-1}$. Perchlorate concentrations in 5 bottled waters from PWSs in Japan were in the range of <0.05 to $0.92\,\mu g\,l^{-1}$ and those in the remaining 59 bottled waters (e.g., natural and purified waters) mostly from Japan were in the range of <0.05 to $0.57\,\mu g\,l^{-1}$. Perchlorate concentrations in the bottled waters for sale in China were also reported. Perchlorate concentrations in seven bottled purified waters were found to be $<0.002\,\mu g\,l^{-1}$. Perchlorate concentrations in 21 of 22 bottled natural mineral waters were in the range of <0.002 to $0.332 \pm 0.017\,\mu g\,l^{-1}$ and that in the remaining 1 was $2.013 \pm 0.015\,\mu g\,l^{-1}$. From the reported data, it appears that perchlorate concentrations in bottled waters are generally low (up to

sub-microgram per liter), with only some samples tested showing levels of several micrograms per liter.

See also: Perchlorate: Human Toxicity.

Further Reading

Asami M, Kosaka K, Yoshida N, Matsuoka Y, and Kunikane S (2008) Occurrence of chlorate and perchlorate in water environment, drinking water and hypochlorite solution. *Journal of Japan Water Works Association* 883: 7–22 (in Japanese).

Bao H and Gu B (2004) Natural perchlorate has a unique oxygen isotope signature. *Environmental Science and Technology* 38: 5073–5077.

Brandhuber P and Clark S (2005) *Perchlorate Occurrence Mapping*, American Water Works Association. http://www.awwa.org/files/Advocacy/PerchlorateOccurrenceReportFinalb02092005.pdf (accessed December 2009).

Dasgupta PK, Dyke JV, Kirk AB, and Jackson WA (2006) Perchlorate in the United States. Analysis of relative source contributions to the food chain. *Environmental Science and Technology* 38: 6608–6614.

Dasgupta PK, Martinelango PK, Jackson WA, et al. (2005) The origin of naturally occurring perchlorate: The role of atmospheric processes. *Environmental Science and Technology* 39: 1569–1575.

El Aribi H, Le Blanc YJC, Antonsen S, and Sakuma T (2006) Analysis of perchlorate in foods and beverages by ion chromatography coupled with tandem mass spectrometry (IC-ESI-MS/MS). *Analytica Chimica Acta* 567: 39–47.

Hogue C (2003) Rocket-fueled river. *Chemical and Engineering News* 81: 37–46. http://pubs.acs.org/cen/coverstory/8133/8133perchlorates.html (accessed July 2010).

Interstate Technology and Regulatory Council (ITRC) Perchlorate Team (2005). *Perchlorate: Overview of Issues, Status, and Remedial Options*. http://www.itrcweb.org/Documents/PERC-1.pdf (accessed December 2009).

Kosaka K, Asami M, Matsuoka Y, Kamoshita M, and Kunikane S (2007) Occurrence of perchlorate in water purification plants in Tone River Basin. *Journal of Japan Society on Water Environment* 30: 361–367. (in Japanese).

Kosaka K, Asami M, Matsuoka Y, Kamoshita M, and Kunikane S (2007) Occurrence of perchlorate in drinking water sources of metropolitan area in Japan. *Water Research* 41: 3474–3482.

Liu YJ, Mou SF, Lin AW, Chui JH, and Du B (2004) Investigation of bromate, haloacetic acids and perchlorate in Beijing's drinking water. *Environmental Science* 25: 51–55. (in Chinese).

Massachusetts Department of Environmental Protection (2005). *The Occurrence and Sources of Perchlorate in Massachusetts (Draft Report)*. http://www.mass.gov/dep/cleanup/sites/percsour.pdf (accessed December 2009).

National Research Council (2005) *Health Implications of Perchlorate Ingestion*. Washington, DC: National Academies Press.

Parker DR, Seyfferth AL, and Reese BK (2008) Perchlorate in groundwater: A synoptic survey of "pristine" sites in the coterminous United States. *Environmental Science and Technology* 42: 1465–1471.

Plummer LN, Bohlke JK, and Doughten MW (2006) Perchlorate in pleistocene and holocene groundwater in north-central New Mexico. *Environmental Science and Technology* 40: 1757–1763.

Quiñones Q, Oh JE, Vanderford B, et al. (2007) Perchlorate assessment of the Nakdong and Yeongsan watersheds, Republic of Korea. *Environmental Toxicology and Chemistry* 26: 1349–1354.

Rajagopalan S, Anderson TA, Fahlquist L, et al. (2006) Widespread presence of naturally occurring perchlorate in high plains of Texas and New Mexico. *Environmental Science and Technology* 40: 3156–3162.

Shi Y, Zhang P, Wang Y, et al. (2007) Perchlorate in sewage sludge, rice, bottled water and milk collected from different areas in China. *Environment International* 33: 955–962.

Snyder SA, Vanderford BJ, and Rexing DJ (2005) Trace analysis of bromate, chlorate, iodate, and perchlorate in natural and bottled waters. *Environmental Science and Technology* 39: 4586–4593.

The Department of Defense Environmental Data Quality Workgroup (2006). *DoD Perchlorate Handbook*, Revision 1, Change 1. http://www.fedcenter.gov/_kd/Items/actions.cfm?action=Show&item_id=8172&destination=ShowItem.

Tock RW, Jackson WA, Anderson T, and Arunagiri S (2004) Electrochemical generation of perchlorate ions in chlorinated drinking water. *Corrosion* 60: 757–763.

United States Environmental Protection Agency, Region 9 (2006) *Perchlorate Monitoring Results Henderson, Nevada to the Lower Colorado River December 2005 Report*. Available at: http://www.epa.gov/fedfac/pdf/perrpt12_05.pdf (accessed December 2009).

United States Food and Drug Administration (2004-05) *Exploratory Survey Data on Perchlorate in Food*. http://www.fda.gov/Food/FoodSafety/FoodContaminantsAdulteration/ChemicalContaminants/Perchlorate/ucm077685.htm.

Wilkin RT, Fine DD, and Burnett NG (2007) Perchlorate behavior in a municipal lake following fireworks displays. *Environmental Science and Technology* 41: 3966–3971.

Relevant Websites

http://www.cdph.ca.gov/CERTLIC/DRINKINGWATER/Pages/Perchlorate.aspx
California, Department of Public Health.

http://www.mass.gov/dep/water/drinking/percinfo.htm
Massachusetts, Department of Environmental Protection.

http://www.epa.gov/OGWDW/ucmr/data.html
United States Environmental Protection Agency.

http://www.epa.gov/fedfac/documents/perchlorate_links.htm#key
United States Environmental Protection Agency Federal Facilities Restoration and Reuse Office.

Separation and Purification Technology 107 (2013) 79–84

Contents lists available at SciVerse ScienceDirect

Separation and Purification Technology

journal homepage: www.elsevier.com/locate/seppur

Adsorptive virus removal with super-powdered activated carbon

Taku Matsushita *, Hideaki Suzuki, Nobutaka Shirasaki, Yoshihiko Matsui, Koichi Ohno

Graduate School of Engineering, Hokkaido University, N13W8, Sapporo 060-8628, Japan

ARTICLE INFO

Article history:
Received 17 April 2012
Received in revised form 10 January 2013
Accepted 15 January 2013
Available online 31 January 2013

Keywords:
Bacteriophage
Drinking water treatment
Hydrophobicity
Zeta potential

ABSTRACT

We investigated the removal of bacteriophages by adsorption on commercially available powdered activated carbon (N-PAC, median diameter >10 μm) and super-powdered activated carbon (S-PAC, median diameter 0.7–2.8 μm). N-PACs failed to remove the virus in Milli-Q water buffered with 100 μM Ca^{2+}, but some S-PACs successfully removed it under the same condition. Three factors contributed substantially to virus removal: a smaller electrophoretic repulsive force between the virus and the PAC particles, a large proportion of pores 20–50 nm in diameter, and a greater hydrophobicity of the virus surface.

1. Introduction

The development of detection techniques based on molecular biology has enabled us to detect fragments of viral genomes in environmental waters, including drinking water sources, highlighting the need to ensure the removal of viruses at drinking water treatment plants. Although disinfecting water with hypochlorite ensures the biological safety of the finished water, the risk of virus infections can be reduced by physicochemical treatments such as coagulation–sedimentation–sand filtration; physical sieving processes such as ultrafiltration, nanofiltration, and reverse osmosis; and ozonation and UV irradiation.

Activated carbon adsorption is widely used to treat drinking water in Japan. Granular activated carbon (GAC) is used in combination with ozonation for removing byproducts derived from the oxidative decomposition of organic matter. Powdered activated carbon (PAC) is seasonally applied with excellent results for removing chemicals with an earthy–musty odor and pesticides. It has also been tested for virus removal. Adsorption experiments with a GAC-loaded (20 × 50 mesh, equivalent to 297–853 μm) column-type reactor removed only 24–50% of poliovirus [1]. Worse, GAC filtration did not remove bacteriophage MS2 [2]. These results indicate that GAC is not suitable for substantial virus removal within the contact time allowed in actual drinking water treatment, probably on account of a low rate of adsorption of virus. Indeed, only 70% of bacteriophage T4 was removed by activated carbon (300–425 μm) after 2 h of contact time [3]. Accordingly, effective virus removal by activated carbon will require a longer contact time, an extremely high dose of activated carbon, or both.

Reducing the particle size of activated carbon increases the rate of adsorption [4,5], because the travel distance for intraparticle radial diffusion is reduced and the specific surface area per adsorbent mass is increased [6]. Pulverizing activated carbon would therefore overcome the problems of slow adsorption kinetics, but the PAC particle size was previously limited to about 5 μm. Recent advances in nanotechnology now enable pulverization down to submicron or nanometer size ranges at a reasonable cost, producing super-powdered activated carbon (S-PAC) [7–9]. As S-PAC might improve virus removal, our objectives were to investigate the effect of pulverization of PAC particles on virus removal and the factors contributing to virus removal.

2. Materials and methods

2.1. Activated carbon

We tested 11 commercially available, thermally activated, normal PACs (N-PACs): 9 wood-based, 2 coconut-based, and 1 coal-based (Table 1). To prepare the S-PACs, we ground the N-PACs in a wet bead mill (Metawater Co., Ltd., Tokyo, Japan). We used both sets of materials to determine the effects of particle size on virus removal by adsorption. The PACs were dried in an oven at 105 °C and stored in a desiccator before use. They were then made into 5% slurries in Milli-Q water (Milli-Q Advantage, Millipore Corp., Billerica, MA, USA) and placed under vacuum to remove any air from the pores. The slurries were stored at 4 °C before dilution for use in the experiments. The particle size distributions were determined by laser scattering (LMS-30 Micron Sizer; Seishin Enterprise Co., Ltd., Tokyo, Japan). The surfaces of the N-PACs were observed by scanning transmission electron microscopy (SEM, JSM-7400F; JEOL Ltd., Tokyo, Japan).

* Corresponding author. Tel./fax: +81 11 706 7279.
E-mail address: taku-m@eng.hokudai.ac.jp (T. Matsushita).

1383-5866/$ - see front matter © 2013 Published by Elsevier B.V.
http://dx.doi.org/10.1016/j.seppur.2013.01.017

Table 1
Activated carbon used.

	Raw material	Median diameter (μm)		Key characteristics of S-PAC						
				Specific surface area[a] (m^2/g)	Element contents[b] (%)				Functional group[c]	
		S-PAC	N-PAC		C	O	N	S	Acidic	Basic
Wood-1	Wood	0.69	13.24	1145 ± 33	85.3 ± 0.6	7.05 ± 0.97	0.14 ± 0.01	0.10 ± 0.02	350 ± 9	790 ± 21
Wood-2	Wood	0.83	4.5	873 ± 39	80.0 ± 1.5	6.70 ± 0.51	0.25 ± 0.02	0.20 ± 0.02	193 ± 58	711 ± 139
Wood-3	Wood	1.49	NA	NA	NA	NA	NA	NA	NA	NA
Wood-4	Wood	0.66	NA	NA	84.6 ± 0.8	6.72 ± 0.11	0.15 ± 0.00	0.11 ± 0.03	NA	NA
Wood-5	Wood	2.79	NA	NA	NA	NA	NA	NA	NA	NA
Wood-6	Wood	1.38	NA	NA	NA	NA	NA	NA	NA	NA
Wood-7	Wood	2.20	NA	NA	NA	NA	NA	NA	NA	NA
Wood-8	Wood	0.93	11.46	1174 ± 14	81.9 ± 0.6	8.24 ± 0.48	0.20 ± 0.01	0.15 ± 0.02	351 ± 22	780 ± 56
Wood-9	Wood	1.65	0.6	NA	NA	NA	NA	NA	NA	NA
Coconut-1	Coconut shell	0.67	NA	NA	88.1 ± 0.5	5.95 ± 0.41	0.16 ± 0.02	0.11 ± 0.03	425 ± 34	329 ± 35
Coconut-2	Coconut shell	0.65	19.13	1215 ± 149	89.1 ± 0.2	5.30 ± 0.10	0.18 ± 0.04	0.06 ± 0.02	433 ± 16	582 ± 29
Coal-1	Coal	0.67	NA	NA	79.2 ± 0.3	10.62 ± 0.24	0.38 ± 0.00	0.55 ± 0.01	757 ± 36	366 ± 36
Determination coefficient (r^2) between logarithmic virus removal indicated in Fig. 2				0.38	0.01	0.06	0.06	0.06	0.08	0.10

NA – not applicable.
[a] Determined with BET.
[b] Measured with an elemental analyzer (Vario EL III, Elementar Analysensysteme GmbH, Hanau, Germany).
[c] Measured with Boehm titration [28,29].

2.2. Viruses

As model viruses we used two bacteriophages, Qβ (NBRC 20012) and MS2 (NBRC 20015), obtained from the Biological Resource Center (NBRC) of the National Institute of Technology and Evaluation (Chiba, Japan). The diameters of Qβ and MS2 are 23.5 ± 0.8 nm and 22.5 ± 1.0 nm, respectively [10]. The viruses were propagated for 22–24 h at 37 °C in *Escherichia coli* F^+ (NBRC 13965) obtained from NBRC. The cultures were centrifuged at 3000*g* for 10 min and then filtered through a 0.45-μm pore-size membrane (cellulose acetate; DISMIC-25cs; Toyo Roshi Kaisya, Ltd., Tokyo, Japan). The filtrate was purified twice in a centrifugal filter device (molecular weight cutoff: 100,000; Centriplus-100; Millipore Corp., Billerica, MA, USA) to prepare virus stock solution. Virus concentrations were measured by the plaque-forming unit (PFU) method according to the agar overlay method [11] using the bacterial host *E. coli* F^+. Average plaque counts of triplicate plates prepared from one sample gave the virus concentration.

2.3. Batch adsorption test

Milli-Q water was buffered with 424 μM $NaHCO_3$ to give the equivalent of 20 mg-$CaCO_3$/L of alkalinity (buffered Milli-Q water). The buffered Milli-Q water was supplemented with 0, 100, 200, 300, 400, or 500 μM $CaCl_2$. In a square beaker, 500 mL of solution was adjusted to pH 6.8 with HCl, and either Qβ or MS2 was added to give 10^6 PFU/mL. PAC was added at 20 mg/L and the suspension was continuously stirred at $G = 200\ s^{-1}$ with a jar tester. Samples were withdrawn at 0, 1, 2, 4, and 8 h and filtered through a membrane (ϕ = 0.2 μm, PTFE; Toyo Roshi Kaisya) to remove the PAC particles. The virus concentration in the permeate was measured by the PFU method.

2.4. Electrophoretic mobility

All solutions were held for 1 day at 20 °C for the pH to stabilize. Just before measurement, each S-PAC or virus was suspended in the solution at ~20 mg/L or 10^9 PFU/mL, respectively. The electrophoretic mobility of S-PACs and viruses was measured with an electrophoretic light-scattering spectrophotometer (Zetasizer Nano ZS, 532 nm green laser; Malvern Instruments Ltd., Malvern, Worcestershire, UK) at 25 °C and at a 17° measurement angle.

2.5. Pore size distribution analyses of PACs

Pore size was analyzed by nitrogen gas adsorption at 77 K with an automated gas sorption analyzer (Autosorb-iQ-MP; Quantachrome Instruments, Boynton Beach, FL, USA). Pore size distributions were determined by a combination of two widely accepted models: the DFT model for the pore size distribution of micropores (<2 nm) and the BJH theory for the volumes of mesopores and macropores (>2 nm).

2.6. Virus hydrophobicity

Hydrophobicity was estimated by the bacterial adhesion to hydrocarbon (BATH) method [12]. Virus was added to 3 mL of buffered Milli-Q water at a final concentration of ~10^8 PFU/mL at pH 7.0. The solution was supplemented with 0.25 mL of solvent (*n*-hexadecane, *n*-octane, or *p*-xylene). The solution was intensely vortexed for 2 min, and then rested for 15 min at room temperature to allow the solvent and water to separate. The virus concentration in the water phase was measured by real-time PCR [13]. A decrease in virus concentration was used as a measure of the virus surface hydrophobicity [12].

3. Results and discussion

3.1. Comparison of virus removal between N-PACs and S-PACs

Virus removal increased with time even without PAC dosing (black circles), probably owing to spontaneous inactivation (Fig. 1). N-PACs (white circles) of wood-8 and coconut-2 showed the same result as the control. S-PACs of wood-8 and coconut-2 (gray circles) also showed the same result, even though their outer surface areas per unit mass were 12.3× and 29.4× those of the N-PACs, respectively. N-PAC of wood-1 removed some virus. In contrast, S-PAC of wood-1, with 19.2× the outer surface area of the N-PAC, caused a monotonic decrease in virus concentration with contact time, reaching a 4 log reduction after 8 h. Our result appears to disagree with that of Powell et al. [14], who reported

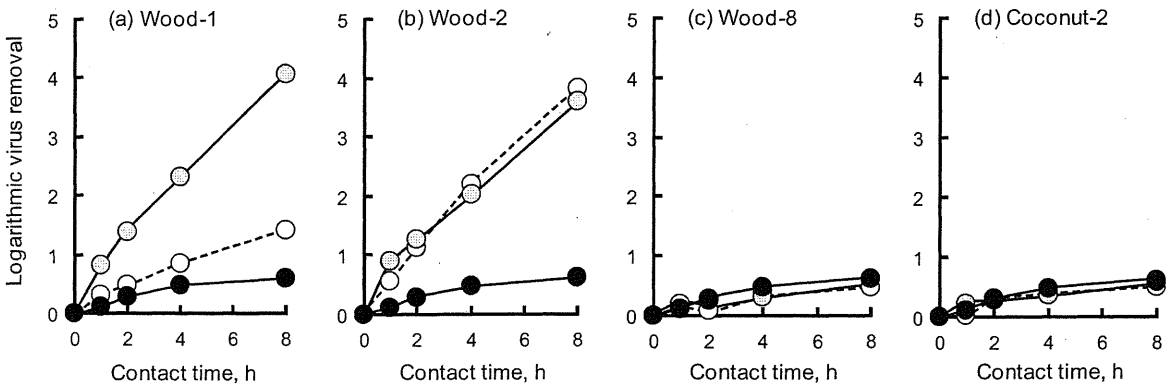

Fig. 1. Changes in virus (Qβ) removal with contact time (Ca^{2+} = 100 μM). Gray, white and black circles indicate SPAC, N-PAC and control, respectively.

that the adsorption of bacteriophage MS2 to a GAC reached equilibrium in 3 h. However, whereas they found that the amount of virus *adsorbed* had plateaued (>99% removal), we monitored the concentration of virus in the *liquid phase*, which might have decreased further even after 99% of the virus was adsorbed. N-PAC of wood-2 removed virus at the same extent as S-PAC of wood-1, possibly because the particle size of N-PAC of wood-2 was much smaller than those of other N-PACs. Virus removal with S-PAC of wood-2 was almost the same to that with the N-PAC, possibly because the N-PAC was small enough to remove the virus and its outer surface area was not so much increased with the pulverization (5.4×). The pulverization enhanced the adsorptive removal by the wood-1 PAC, but not by the wood-2, wood-8 and coconut-2 PACs. Overall, the effect of pulverization on virus removal might depend on the intrinsic characteristics of the PACs.

3.2. Effects of median diameter and PAC source on virus removal

We expected that finer PACs would remove more virus. However, different S-PACs with the same median diameter of ~0.7 μm showed very different removals of virus: wood-1 and wood-2 S-PACs achieved a removal of ~4 orders of magnitude (4 logs), whereas the other S-PACs achieved a removal of <2 logs (Fig. 2). Virus removal may be influenced by many factors such as raw material, specific surface area, element content, surface functional group, pore size distribution and surface charge. Nevertheless, as the capacity of the wood-based PACs varied widely from 0.5 to 4 logs, and a coconut-based PAC removed more virus than some wood-based PACs, the difference in virus removal seems to be due to more than the raw materials. The inherent characteristics of PAC listed in Table 1, i.e. specific surface area, element content and surface functional group, obviously had no relationship with the virus removal ($r^2 < 0.4$); other inherent factors most likely had influence on the adsorptive removal. To investigate the factors affecting the removal, we made a comparison in the following sections among two S-PACs that exhibited the highest virus removal (i.e. wood-1 and wood-2 S-PACs) and 2 S-PACs that had similar particle diameters to the superior S-PACs but exhibited the lowest virus removal (i.e. wood-8 and coconut-2 S-PACs).

3.3. Effect of surface charge of PACs on virus removal

When virus and S-PACs were dispersed in buffered Milli-Q water without Ca^{2+}, both particles were highly negatively charged, and the electrostatic repulsive force between them, measured as electrophoretic mobility, was high (Fig. 3). As the Ca^{2+} concentra-

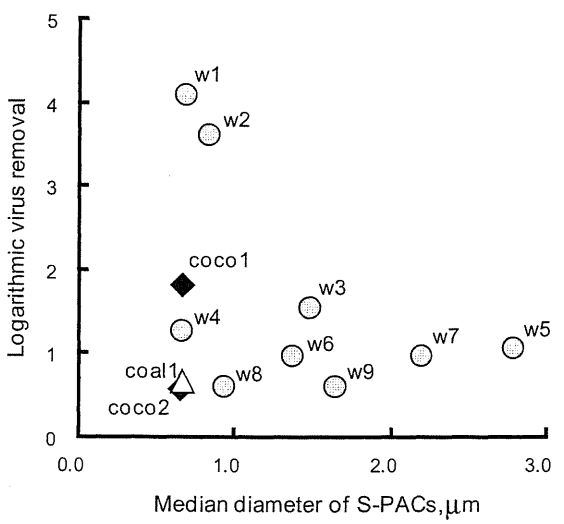

Fig. 2. Relationship between median diameter of S-PACs and virus removal (contact time = 8 h, Ca^{2+} = 100 μM). Circles, diamonds and triangle represent wood-, coconut- and coal-based SPACs. Logarithmic virus removals for wood-1, wood-2, wood-8 and coconut-2 S-PACs were averaged values of two experiments with too small deviations to see, while those for other S-PACs were obtained in one experiment.

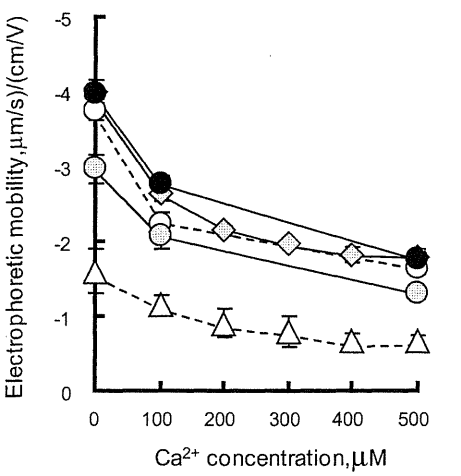

Fig. 3. Electrophoretic mobility of Qβ and S-PACs at different concentrations of Ca^{2+}. White, gray and black circles, gray diamonds and white triangles indicate wood-1, wood-2, wood-8, coconut-2 and Qβ, respectively. Error bars indicate SD of 10 measurements.

tion increased, the electrophoretic mobilities of both virus and S-PACs decreased. In general, an increase in ionic strength compresses the diffuse layer of ions surrounding a charged particle, decreasing the extent of the charge. This behavior has been seen before in viruses [15–18]. Our results support this.

The repulsion energy (V_R) of the electrical double layer between two closely spaced spheres is described as follows [19]:

$$V_R = 2\pi\varepsilon\zeta_1\zeta_2\frac{d_1 d_2}{d_1 + d_2}\exp(-\kappa h) \quad (1)$$

where ε is the permittivity of the medium, ζ_1 and ζ_2 are the zeta potentials of the spheres, d_1 and d_2 are the diameters of the spheres, and h is the minimum surface-to-surface separation between the spheres. κ is the Debye–Hückel reciprocal length:

$$\kappa = \sqrt{\frac{e^2\sum n_{i0}z_i^2}{\varepsilon kT}} \quad (2)$$

where e is the elementary charge, n_0 is the number concentration of ions in the bulk solution, z is the valency of the ion, k is the Boltzmann constant, and T is the absolute temperature. When virus and S-PAC were spaced 0.2 nm apart, as the Ca^{2+} concentration increased, the repulsion decreased (Fig. 4). Virus removal improved from 1–3 logs at 0 μM-Ca^{2+} to 3–6 logs at 500 μM-Ca^{2+}. Thus, virus removal was enhanced as the repulsion decreased. A higher ionic strength compresses the electrical double-layer of charged particles, reducing the electrostatic repulsion between like-charged particles and enabling the particles to move nearer to each other [17,21,22]. The adsorption of the virus onto the S-PAC was most likely hampered by the electrostatic repulsive force between them. Therefore, reducing the repulsion by increasing the ionic strength improved virus removal. One explanation is that the positive ions shield the negative charges on the surfaces of the adsorbate and the adsorbent, decreasing the net electrostatic repulsion between the particles [16,18,20,23]. Or Ca^{2+} may electrically adsorb to a negatively charged moiety of both adsorbate and adsorbent concurrently, forming a cation bridge to link the like-charged particles [18,23,24].

Fig. 5 shows the relationship between the virus removal and the electrical double layer repulsion energy. Virus removal tended to increase as the repulsive force decreased, but the removal performances were different among s-PACs. Wood-1 S-PAC exhibited superior virus removal across all repulsion energy range: the virus removal with wood-1 S-PAC was always greater than those with other S-PACs tested even in the range in which the repulsive force

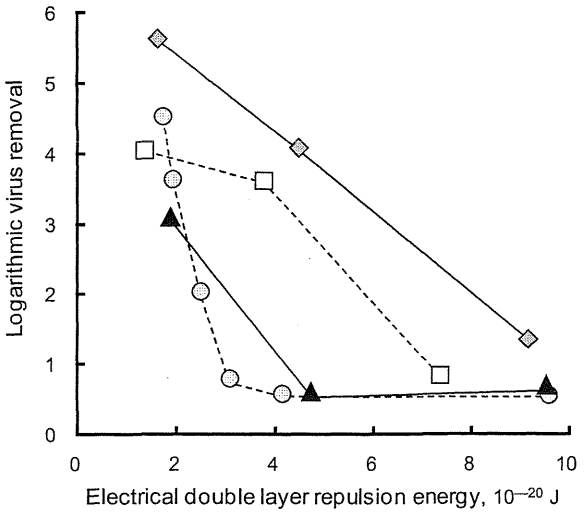

Fig. 5. Relationship between virus removal (Qβ, contact time = 8 h) and repulsion energy of electrical double layer (0.2 nm distance). Gray diamonds, white squares, black triangles and gray circles indicate wood-1, 2, 8 and coconut-2, respectively. Repulsion energy was controlled by Ca^{2+} concentration.

working between the virus and S-PAC particles was the same. These observations mean that the electrostatic repulsion can explain the extent of virus removal by each S-PAC under different ionic conditions, but not the difference between different types of PAC.

The logarithmic virus removals of wood-1 and wood-2 S-PACs linearly increased with decrease in the electrical double layer repulsion energy. In contrast, the virus removals of wood-8 and coconut-2 S-PACs did not change even when the repulsion energy decreased down from 10×10^{-20} to 3×10^{-20} J, but seem to increase drastically when the repulsion energy was smaller than 3×10^{-20} J. Possible reason for this observation is discussed in the following section.

3.4. Effect of pore size distribution of PACs on virus removal

SEM observations revealed that the wood-1 and wood-2 S-PACs, which could remove virus effectively, had a rough surface with many mesopores 20–50 nm in diameter (Photo 1). In contrast,

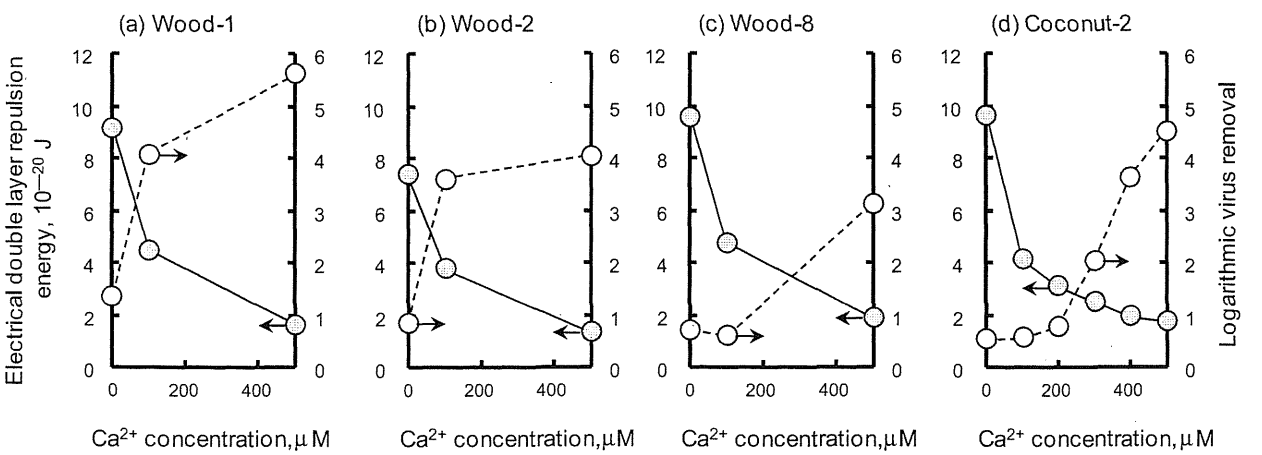

Fig. 4. Changes in repulsion energy of electrical double layer between the virus and S-PACs at 0.2 nm distance, and virus removal (Qβ, contact time = 8 h) with increase in Ca^{2+} concentration. Gray and white circles indicate the electrical double layer repulsion energy and the logarithmic virus removal, respectively.

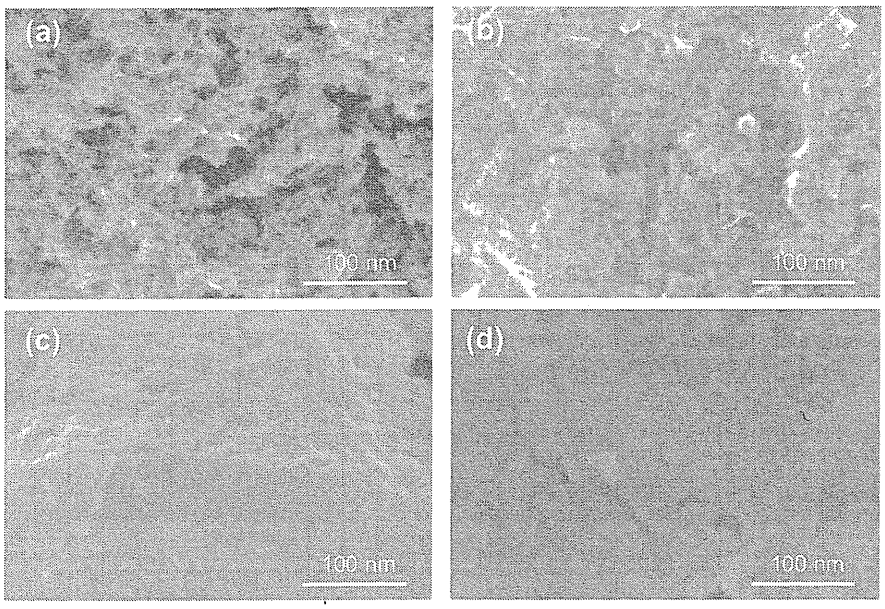

Photo 1. SEM images of S-PAC surfaces: (a) wood-1; (b) wood-2; (c) wood-8; and (d) coconut-2.

Table 2
Comparison in pore volume among S-PACs.

Pore diameter (nm)	Wood-1	Wood-2	Wood-8	Coconut-2
1–2	0.203	0.123	0.206	0.177
2–3	0.040	0.040	0.056	0.030
3–5	0.071	0.091	0.053	0.044
5–10	0.063	0.088	0.038	0.037
10–20	0.044	0.066	0.025	0.028
20–50	0.035	0.039	0.017	0.022

Table 3
Logarithmic removals of Qβ and MS2 with S-PACs (contact time = 8 h, Ca^{2+} = 100 μM).

	Wood-1	Wood-2
Qβ	4.1	3.6
MS2	3.0	2.9

the wood-8 and coconut-2 S-PACs, whose virus removal was poor, had a relatively smooth surface with no mesopores. With a diameter of ~23 nm, the virus cannot pass through pores smaller than this. The nearer the diameter of an adsorbate molecule is to the pore size of an adsorbent, the greater is the attraction [25]. Therefore, the wood-1 and wood-2 S-PACs, with pores 20–50 nm wide, offered good conditions for the virus to settle in, and so removed it effectively. This most likely contributed to the difference of behaviors of viruses in the relationship between the logarithmic virus removal and the electrical double layer repulsion energy indicated in Fig. 5: the wood-1 and wood-2 could easily capture the virus particles with many suitable pores for the virus particles to settle in even under the large repulsion energy that prevented the adsorption of the virus particles to the wood-8 and coconut-2 S-PACs. At this moment, the reason why the virus removals of wood-8 and coconut-2 S-PACs increased drastically with the decrease in the repulsion energy is not clear.

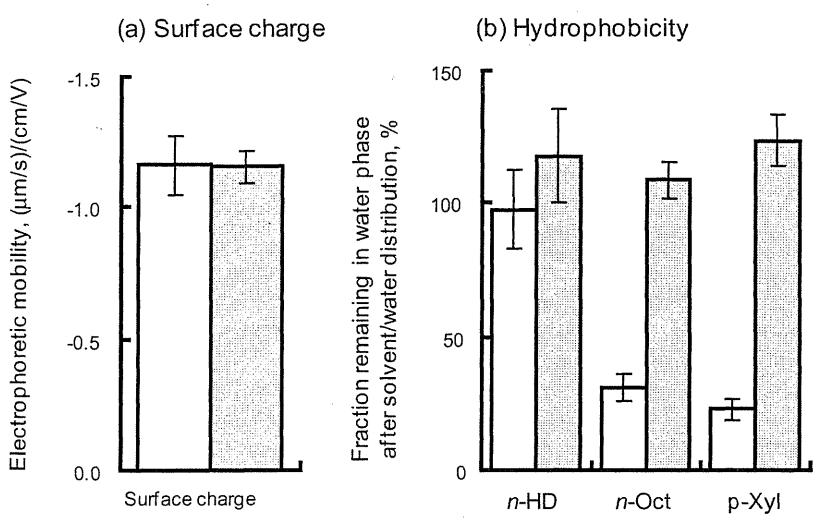

Fig. 6. Comparison of (a) surface charge and (b) hydrophobicity between Qβ and MS2. White and gray columns represent Qβ and MS2, respectively. *n*-HD, *n*-hexadecane; *n*-Oct, *n*-octanol; p-Xyl, p-xylene. Error bars in (a) and (b) indicate SD of 30 and 5 measurements, respectively.

Pore size measurements clearly show that the wood-1 and wood-2 S-PACs had larger pore volume at 20–50 nm than the wood-8 and coconut-2 S-PACs (Table 2); the pore volumes of the high-virus-adsorbable S-PACs were 1.8–2.0 times as much as the averaged pore volume of the low-virus-adsorbable S-PACs. These results agree well with the SEM observations, supporting the hypothesis that the pore size distribution of the S-PACs contributed greatly to virus removal.

3.5. Effect of hydrophobicity of virus on virus removal

The removal of bacteriophage MS2 was ~1 log less than that of Qβ by both wood-1 and wood-2 S-PACs (Table 3). Although the molecular size of an adsorbate controls accessibility to the pores of the activated carbon [26], the diameters of the Qβ and MS2 are almost the same (~23 nm), so this does not explain the difference in removal. Likewise, although the surface charges of viruses depend on the chemistry of their surface proteins, we found no difference in the surface charge between the two viruses (Fig. 6a). Instead, they differed in hydrophobicity (Fig. 6b): MS2 remained in the water phase of all solvent combinations tested, indicating that it has a hydrophilic surface. In contrast, Qβ largely transferred to the solvent phase when *n*-octane and p-xylene were used. This result indicates that the surface of Qβ is more hydrophobic than that of MS2, in agreement with a previous report [27]. Thus, the more hydrophobic the surface of the virus particles is, the greater the virus removal would be expected. As shown in Section 3.3, reducing the surface charge of the activated carbons improved virus removal. The reduction in the surface charge may provide more hydrophobic surface on the carbon apparently, because the reduction allows negatively charged adsorbates to move nearer to the graphite structure on the carbon. Adding to the reduction in the electrophoretic repulsive force, the apparent increase in hydrophobicity of the carbon surface most likely contributed to the high virus removal. Likewise, the hydrophobicity of the viruses contributed to the high removal: the virus having more hydrophobic surface was removed more greatly with the activated carbons.

4. Conclusions

(1) Electrophoretic repulsive force contributed greatly to virus removal: the smaller the repulsion between virus and PAC particles, the greater the virus removal.
(2) The pore size distribution of the PAC contributed greatly to virus removal: PACs with a large volume of pores 20–50 nm in diameter removed virus effectively.
(3) The hydrophobicity of the virus surface contributed greatly to virus removal: the more hydrophobic the surface, the greater the virus removal.
(4) To enhance adsorptive virus removal, activated carbons must have a less negative surface charge and a large volume of pores 20–50 nm wide.

Acknowledgments

Makoto Kobuke and Tomoko Aki made efforts for the experiments on the virus hydrophobicity and the surface functional group of the activated carbons, respectively. This research was supported in part by a Grant-in-Aid for the Encouragement of Young Scientists (2010) from the Ministry of Education, Culture, Sports, Science and Technology of Japan; a Grant-in-Aid (2010) from the Ministry of Health, Labor and Welfare of Japan; and a Kurita Water and Environment Foundation Research Grant (2009).

References

[1] C.P. Gerba, M.D. Sobsey, C. Wallis, J.L. Melnick, Adsorption of poliovirus onto activated carbon in wastewater, Environ. Sci. Technol. 9 (1975) 727–731.
[2] W.A. Hijnen, G.M.H. Suylen, J.A. Bahlman, A. Brouwer-Hanzens, G.J. Medema, GAC adsorption filters as barriers for viruses, bacteria and protozoan (oo)cysts in water treatment, Water Res. 44 (2010) 1224–1234.
[3] P.P. Oza, M. Chaudhuri, Removal of viruses from water by sorption on coal, Water Res. 9 (1973) 707–712.
[4] S.J. Randtke, V.L. Snoeyink, Evaluating GAC adsorptive capacity, J. AWWA 75 (1983) 406–413.
[5] I.N. Najm, V.L. Snoeyink, M.T. Suidan, C.H. Lee, Y. Richard, Effect of particle size and background natural organics on the adsorption efficiency of PAC, J. AWWA 82 (1990) 65–72.
[6] H. Sontheimer, J.C. Crittenden, R.S. Summers, Activated Carbon for Water Treatment, second ed., DVGW-Forschungsstelle, Karlsruhe, Germany, 1988.
[7] Y. Matsui, R. Murase, T. Sanogawa, N. Aoki, S. Mima, T. Inoue, T. Matsushita, Rapid adsorption pretreatment with submicron powdered activated carbon particles before microfiltration, Water Sci. Technol. 51 (6–7) (2005) 249–256.
[8] Y. Matsui, T. Sanogawa, N. Aoki, S. Mima, T. Matsushita, Evaluating submicron-sized activated carbon adsorption for microfiltration pretreatment, Water Sci. Technol.: Water Supply 6 (1) (2006) 149–155.
[9] Y. Matsui, N. Ando, H. Sasaki, T. Matsushita, K. Ohno, Branched pore kinetic model analysis of geosmin adsorption on super-powdered activated carbon, Water Res. 43 (2009) 3095–3103.
[10] N. Shirasaki, T. Matsushita, Y. Matsui, M. Kobuke, K. Ohno, Comparison of removal performance of two surrogates for pathogenic waterborne viruses, bacteriophage Qβ and MS2, in a coagulation–ceramic microfiltration system, J. Membrane Sci. 326 (2009) 564–571.
[11] M.H. Adams, Bacteriophages, Interscience, New York, NY, USA, 1959.
[12] M. Rosenberg, D. Gutnick, E. Rosenberg, Adherence of bacteria to hydrocarbons: a simple method for measuring cell-surface hydrophobicity, FEMS Microbiol. Lett. 9 (1980) 29–33.
[13] N. Shirasaki, T. Matsushita, Y. Matsui, A. Oshiba, K. Ohno, Estimation of norovirus removal performance in a coagulation-rapid sand filtration process by using recombinant norovirus VLPs, Water Res. 44 (2010) 1307–1316.
[14] T. Powell, G.M. Brion, M. Jagtoyen, F. Derbyshire, Investigating the effect of carbon shape on virus adsorption, Environ. Sci. Technol. 34 (2000) 2779–2783.
[15] S.L. Penrod, T.M. Olson, S.B. Grant, Whole particle microelectrophoresis for small viruses, J. Colloid Interface Sci. 173 (1995) 521–523.
[16] J.A. Redman, S.B. Grant, T.M. Olson, J.M. Adkins, J.L. Jackson, M.S. Castillo, W.A. Yanko, Physicochemical mechanisms responsible for the filtration and mobilization of a filamentous bacteriophage in quartz sand, Water Res. 33 (1999) 43–52.
[17] B. Yuan, M. Pham, T.H. Nguyen, Deposition kinetics of bacteriophage MS2 on a silica surface coated with natural organic matter in a radial stagnation point flow cell, Environ. Sci. Technol. 42 (2008) 7628–7633.
[18] S.E. Mylon, C.I. Rinciog, N. Schmidt, L. Gutierrez, G.C.L. Wong, T.H. Nguyen, Influence of salts and natural organic matter on the stability of bacteriophage MS2, Langmuir 26 (2010) 1035–1042.
[19] J. Gregory, Particles in Water: Properties and Processes, CRC Press, Boca Raton, FL, USA, 2006.
[20] J.C. Lance, C.P. Gerba, Effect of ionic composition of suspending solution on virus adsorption by a soil column, Appl. Environ. Microbiol. 47 (1984) 484–488.
[21] D.G. Jewett, T.A. Hilbert, B.E. Logan, R.G. Arnold, R.C. Bales, Bacterial transport in laboratory columns and filters: influence of ionic strength and pH on collision efficiency, Water Res. 29 (1995) 1673–1680.
[22] H. Cao, F.T.C. Tsai, K.A. Rusch, Impact of salinity on MS-2 sorption in saturated sand columns–fate and transport modeling, J. Environ. Eng. 135 (2009) 1041–1050.
[23] J. Zhuang, Y. Jin, Virus retention and transport through Al-oxide coated sand columns: effects of ionic strength and composition, J. Contaminant Hydrol. 60 (2003) 193–209.
[24] M. Pham, E.A. Mintz, T.H. Nguyen, Deposition kinetics of bacteriophage MS2 to natural organic matter: role of divalent cations, J. Colloid Interface Sci. 338 (2009) 1–9.
[25] R.J. Martin, Activated carbon product selection for water and wastewater treatment, Ind. Eng. Chem. Prod. Res. Dev. 19 (1980) 435–441.
[26] C. Moreno-Castilla, Adsorption of organic molecules from aqueous solutions on carbon materials, Carbon 42 (2004) 83–94.
[27] J. Langlet, F. Gaboriaud, J.F.L. Duval, C. Gantzer, Aggregation and surface properties of F-specific RNA phages: implication for membrane filtration processes, Water Res. 42 (2008) 2769–2777.
[28] H.P. Boehm, Some aspects of the surface-chemistry of carbon-blacks and other carbons, Carbon 32 (1994) 759–769.
[29] H.P. Boehm, Surface oxides on carbon and their analysis: a critical assessment, Carbon 40 (2002) 145–149.

Separation and Purification Technology 113 (2013) 75–82

Contents lists available at SciVerse ScienceDirect

Separation and Purification Technology

journal homepage: www.elsevier.com/locate/seppur

Natural organic matter that penetrates or does not penetrate activated carbon and competes or does not compete with geosmin

Yoshihiko Matsui [a,*], Soichi Nakao [b], Tomoaki Yoshida [b], Takuma Taniguchi [b], Taku Matsushita [a]

[a] Faculty of Engineering, Hokkaido University, N13W8, Sapporo 060-8628, Japan
[b] Graduate School of Engineering, Hokkaido University, N13W8, Sapporo 060-8628, Japan

ARTICLE INFO

Article history:
Received 11 August 2012
Received in revised form 12 December 2012
Accepted 8 April 2013
Available online 19 April 2013

Keywords:
Super-fine
Submicron
Powdered activated carbon
Natural organic matter
Water treatment

ABSTRACT

The adverse effect of natural organic matter (NOM) on the capacity of activated carbon to adsorb 2-methylisoborneol (MIB), a compound with an earthy/musty odor, is less severe for submicron-sized powdered activated carbon (SPAC) than for conventionally sized powdered activated carbon (PAC) [11]. In this study the NOM effect was confirmed, and the mechanism responsible for the effect was investigated by studies with another malodorous compound, geosmin. The mechanism was investigated with respect to the properties of NOM by simplified equivalent background compound (EBC) estimation and penetration index. Correlations between penetration index values and fractional areas of size-exclusion chromatogram indicated that higher NOM loading on SPAC were associated mainly with a fraction of NOM having a molecular weight (MW) >2 kDa and a chromophoric moiety, which did not diffuse into the inner region of adsorbent particles and instead adsorbed only onto their external surfaces. Therefore SPAC, which has a larger specific surface area per unit mass of adsorbent, adsorbs such high-MW chromophoric NOM to a greater extent than does PAC. However, such NOM does not compete for adsorption sites with geosmin because geosmin adsorbs onto the interior surfaces of adsorbent particles. Contrariwise, NOM with a MW of <2 kDa and with an nonchromophoric moiety penetrates adsorbent particles and adsorbs onto interior surfaces. The estimated EBC concentration and its correlations with both size-exclusion chromatogram fractions and penetration index values indicated the characteristics of the NOM that competes with geosmin to be similar to those of MIB. Chromophoric NOM with a MW of <230 Da competes for adsorption sites with both geosmin and MIB. Beside the nonchromophoric, low-MW (<2 kDa) NOM, such chromophoric, very-low-MW NOM also penetrates adsorbent particles and adsorbs onto interior surfaces. The loading of such NOM is therefore independent of the size of the carbon particles (SPAC or PAC). The NOM effects on geosmin adsorption capacity were therefore found to be similar for SPAC and PAC, despite the fact that more NOM was loaded onto SPAC than PAC. The very-low-MW chromophoric NOM accounted for <2% of the entire NOM.

1. Introduction

Geosmin is a metabolite produced by several classes of microbes, including cyanobacteria and actinomyces, and confers an unpleasant earthy/musty taste and odor to drinking water. Because geosmin has an exceptionally low detention threshold (4 to 10 ng/L) by human taste and smell [1,2], the unpleasant taste and odor can be detected when geosmin is present even in low concentrations, and it can easily affect consumer acceptability. Because drinking water that is aesthetically unacceptable reduces consumer confidence in the water treatment and supply system, the treatment goal for water utilities is to provide drinking water that is not only safe but also acceptable in appearance, taste, and odor.

Adsorption by powdered activated carbon (PAC) is the most conventional treatment method for the removal of micro-pollutants such as geosmin, but the treatment is expensive because of the limited capacity of activated carbon to adsorb geosmin [3]. The presence of natural organic matter (NOM) in untreated water limits the adsorption capacity of activated carbon [4]. NOM is considered to be a target for removal by activated carbon adsorption, but at the same time its loading onto activated carbon reduces the number of adsorption sites available for other compounds, such as geosmin. Because the number of adsorption sites available for adsorptive removal is limited for a given amount of activated carbon, compounds compete for adsorption sites. Because this competition leaves only a few adsorption sites available for compounds present in low concentrations, reducing the concentration of geosmin below its extremely low detention threshold (<10 ng/L) requires large dosages of carbon relative to geosmin concentrations.

* Corresponding author. Tel./fax: +81 11 706 7280.
E-mail address: matsui@eng.hokudai.ac.jp (Y. Matsui).

1383-5866/$ - see front matter © 2013 Elsevier B.V. All rights reserved.
http://dx.doi.org/10.1016/j.seppur.2013.04.009

To improve adsorptive removal efficiency, our research group has proposed the use of submicron-sized super-fine powdered activated carbon (SPAC) [5]. The original concept behind the use of SPAC was to improve the uptake rate of the adsorbate. In fact, adsorptive uptake onto SPAC is very fast, and SPAC is far superior to PAC in removing geosmin and natural organic matter (NOM) in a given contact time [6–8]. Furthermore, the capacity of SPAC to adsorb NOM is higher than that of PAC [5,9]. It has also been reported that the capacity of SPAC and PAC to adsorb 2-methylisoborneol (MIB, another earthy/musty taste and odor compound) decrease to the same extent as a result of NOM loading, although SPAC loads NOM more than PAC [10]. This means that the extra amount of NOM loading on SPAC compared with PAC does not result in an extra reduction of MIB adsorption capacity. The explanation is that the NOM that competes with MIB comprises a small portion of NOM (<2% in dissolved organic carbon, DOC) [11]. It has been reported that the NOM that competes with MIB has a very low MW (<230 Da) and chromophoric properties, and that it adsorbs onto internal pores of activated carbon particles as does MIB, thereby reducing the capacity of activated carbon to adsorb MIB to a similar extent regardless of adsorbent size (SPAC or PAC). The same study has also suggested that the competing NOM has a MW similar to that of the target compound. However, these mechanisms, including the competition between a target compound and the NOM fraction with a similar molecular size, were derived from the results of adsorption experiments with one compound, MIB, in waters containing NOM. Generalization of the mechanisms therefore requires adsorption data for other compounds. Meanwhile, another previous study [9] has suggested that NOM with chromophoric properties is adsorbed onto the external surface of activated carbon particles and is hence adsorbed more on the small particles of SPAC than PAC. These results can be reconciled by hypothesizing that the NOM that adsorbs onto the external surface of activated carbon particles is a high-MW fraction of the chromophoric NOM.

The results of adsorption experiments with various NOMs experimentally verified this hypothesis in the present study. We further investigated the characteristics of the competing NOM and the competition mechanism, which had been reported for MIB, by using another micro-pollutant, geosmin.

2. Materials and methods

2.1. Activated carbon

Commercially available wood-based PAC (Taikou-W, Futamura Chemical Industries Co., Gifu, Japan) was prepared as a slurry in ultrapure water and pulverized to super-fine particles of submicron diameter with a wet bead mill (Metawater Co., Tokyo, Japan). In this paper, we refer to the PAC received directly from the supplier as PAC and the pulverized activated carbon prepared with the wet bead mill as SPAC. The PAC and SPAC were stored as slurries in ultrapure water at 4 °C and used after dilution. Particle size distributions of the activated carbons were determined with a laser-light scattering instrument (LA-700, Horiba, Ltd., Kyoto, Japan) following the addition of a dispersant (0.02 mL of 18% anionic surfactant solution per 200 mL SPAC/PAC sample suspension containing between 0.001% and 0.01% carbon) and a 4-min sonication with ultrasound. Median diameters are 13.5 and 0.86 μm for PAC and SPAC, respectively. BET surface areas were determined with an Autosorb-iQ gas adsorption analyzer (Quantachrome Instruments). BET surface areas are 1070 and 1130 g/m^3 for PAC and SPAC, respectively.

2.2. Water samples

Water samples from Lake Kasumigaura (Ibaraki, Japan) and Lake Hakucho (Hokkaido, Japan) were used as examples of natural waters containing NOM (Table 1S, Supplementary information). After collection and transportation to the laboratory, these samples were filtered through 0.2-μm pore size membrane filters (Hydrophilic PTFE type membrane filter; Toyo Roshi Kaisha, Ltd., Tokyo) and adjusted to a similar DOC concentration of ~1.5 mg-C/L by dilution with ultrapure water (Milli-Q Advantage, Millipore Co.,) amended with salts to obtain a uniform ionic composition. SHA (Suwannee humic acid) waters were prepared by dissolving Suwannee River humic acid in ultrapure water (Milli-Q Advantage, Millipore Co.,) containing inorganic ions added to make the ionic composition similar to that of the Kasumigaura and Hakucho NOM waters.

Stock solutions of geosmin were prepared by dissolving reagent geosmin (Wako Pure Chemical Industries, Ltd., Osaka, Japan) in ultrapure water. Solutions of geosmin in NOM water (NOMW) were prepared by diluting the stock solution of geosmin with the above-described NOMWs to produce geosmin concentrations of about 1 μg/L (5.5 nmol/L). Single-solute solutions of geosmin were prepared by diluting the stock solution of geosmin with organic-free waters (OFWs), which we prepared with ultrapure water containing inorganic ions added to make the ionic composition similar to that of the NOMWs. All waters were filtered through a 0.2-μm pore size membrane filter before use. Geosmin concentrations were analyzed using a Purge and Trap Concentrator Coupled to a GC-MS (GCMS-QP2010 Plus; Shimadzu Corp., Kyoto, Japan; Aqua PT 5000 J, GL Sciences Inc., Tokyo, Japan).

DOC concentrations, measured in sample filtrates with a total organic carbon analyzer (Model 810; Sievers Instruments, Inc., Boulder, CO, USA), served as parameters for bulk NOM quantification. UV absorbance at 260 nm (UV_{260}) was measured with a spectrophotometer (Model UV-240, Shimadzu Corp., Kyoto, Japan) and served as an indicator of chromophoric NOM. The MW distributions of the NOMs were determined by using high performance size exclusion chromatography [HPSEC, HP1100 (Agilent Technologies, Inc., CA, USA); packed column GL-P252 (Hitachi, Ltd.); eluent: 0.02 M Na_2HPO_4 + 0.02 M KH_2PO_4]. Polystyrene sulfonate (weight-average MW 1920, 5180, and 6130 Da) and salicylic acid (138 Da) were used for calibration. The UV_{260} and DOC (Model 810 Turbo; GE Analytical Instruments) of the column effluent were measured continuously.

2.3. Batch adsorption tests

Immediately after addition of a specified amount of SPAC/PAC, the 150-mL vials containing geosmin and/or NOM were shaken and then transferred to a shaker that shook them for one week at a constant temperature of 20 °C. Preliminary experiments confirmed that in one week geosmin adsorption had reached equilibrium and that NOM adsorption equilibrium was almost reached. Control tests were also conducted by using multiple bottles that did not contain carbon to confirm that concentration changes during the long-term mixing were negligible. After the water samples were filtered through a 0.2-μm membrane filter (DISMIC-25HP; Toyo Roshi Kaisha, Ltd., Tokyo), adsorbate (geosmin and NOM) concentrations in the water phase were measured.

3. Results and discussion

3.1. The effect of carbon particle size on geosmin adsorption in the presence of NOM

We conducted geosmin adsorption experiments by using the three NOMWs and the OFW. The capacities of both SPAC and PAC to adsorb geosmin were smaller in all NOMWs than in OFW (Fig. 1S). Ratios of capacities to adsorb geosmin in NOMW vs. OFW at the equilibrium liquid-phase concentration of 100 ng/L

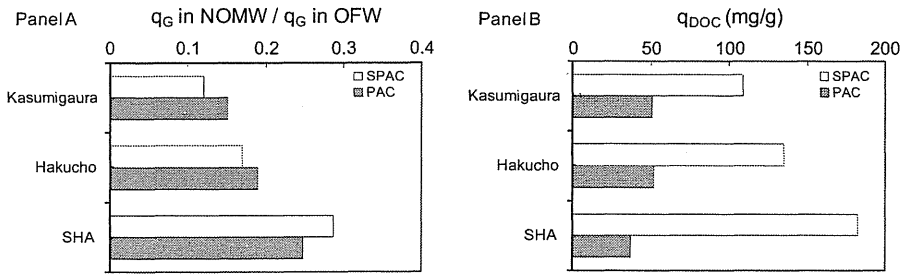

Fig. 1. Panel A: Ratios of geosmin adsorption capacities (designated as "q_G" in the figure) in NOMWs against those in OFW. Panel B: DOC loadings on each carbon. The geosmin adsorption capacities were evaluated by batch adsorption isotherms. Initial and equilibrium geosmin liquid-phase concentrations were 1000 and 100 ng/L, respectively.

are summarized in Fig. 1A. All experiments were conducted at the same initial NOM concentration, but the effects of NOM on geosmin removal were dependent on the type of NOM. The NOM in Kasumigaura water reduced geosmin adsorption to the greatest extent: less than 15% of adsorption capacity remained. However, the amount of DOC in Kasumigaura water that was adsorbed onto carbon was not high compared to the amount of DOC adsorbed from other waters (Fig. 1B). Therefore, the large reduction in geosmin adsorption from Kasumigaura water could not be attributed to the loading of entire NOM. For each of the NOMWs, the ratios of the capacities of SPAC and PAC to adsorb geosmin in NOMW vs. OFW water were similar for SPAC and PAC (Fig. 1A), although SPAC loaded NOM more than PAC (Panel B). This means that the increased amount of NOM loading associated with carbon particle size reduction (from PAC to SPAC) did not result in a further decrease in capacity to adsorb geosmin. Adsorption competition between NOM and geosmin did not become more severe even when NOM loading increased as a result of carbon particle size reduction (from PAC to SPAC).

3.2. Mechanism of NOM competition

The results in Section 3.1 indicate that not all of the NOM competes with geosmin for adsorption sites. Rather, only a portion of NOM seems to be competing with geosmin. Graham et al. [12] estimated the concentration of competing NOM by applying the equivalent background compound (EBC) method and assuming the MW of competing NOM to be 2500 Da: they concluded that the NOM competing with geosmin and MIB was 0.45% of the DOC concentration. The values of EBC parameters, including the initial competing-NOM concentration, are generally determined by a best fit model fit to an experimental isotherm, but the resulting solution for the EBC parameter values is not necessarily unique. In the present study, the amount of competing-NOM loading was estimated by a simplified EBC method, which can avoid the uniqueness problem. When competing NOM is represented by a single hypothetical compound (EBC), the system of micro-pollutant (i.e., geosmin in the present study) in NOMW is modeled as a bi-adsorbate system. The adsorption is described by a Freundlich + IAST (ideal adsorbed solution theory) model.

$$C_G = \frac{q_G}{q_G + q_E}\left(\frac{n_G q_G + n_E q_E}{n_G K_G}\right)^{n_G} \tag{1}$$

where C_G is the liquid-phase concentration of geosmin (nmol/L), q_G is the solid-phase concentration of geosmin (nmol/mg), q_E is the solid-phase concentration of competing NOM (nmol/mg), n_G and K_G are the single-solute Freundlich isotherm exponent and constant, respectively, for geosmin [dimensionless and (nmol/L)/(nmol/mg)$^{1/n}$, respectively], and n_E is the single-solute Freundlich isotherm exponent for EBC (competing NOM) (dimensionless).

With the two assumptions that (i) the solid-phase concentration of the competing NOM is much greater than the solid-phase concentration of the target compound and (ii) the Freundlich exponents of the two adsorbates are not very different, an equation for solid-phase concentration of the competing NOM can be derived [11]:

$$q_E^* \equiv q_E n_E^{\frac{n_G}{n_G-1}} = (n_G K_G)^{\frac{n_G}{n_G-1}}\left(\frac{C_G}{q_C}\right)^{\frac{1}{n_G-1}} \tag{2}$$

where q_E^* is the pseudo solid-phase concentration of competing NOM (nmol/mg).

At high carbon doses in batch adsorption, the mass balances are approximated to;

$$C_{G,0} \cong C_C q_M \tag{3}$$

$$C_{E,0} \cong C_C q_E \tag{4}$$

where $C_{G,0}$ is the initial geosmin concentration (nmol/L); $C_{E,0}$ is the initial concentration of competing NOM (nmol/L).

When carbon doses are high, the isotherm for a micropollutant in natural water can be described by a pseudo-single solute isotherm equation with the same Freundlich exponent as that obtained for the single-solute micropollutant system [13,14]. Therefore,

$$q_G = K_G^* C_G^{\frac{1}{n_G}} \tag{5}$$

where K_G^* is the Freundlich constant describing the geosmin adsorption isotherm obtained in NOMW [(nmol/L)/(nmol/mg)$^{1/n}$].

By substituting Eq. (3) into (5), Eq. (2) becomes;

$$C_{E,0}^* \equiv C_{E,0} n_E^{\frac{n_G}{n_G-1}} = C_{G,0}\left(n_G \frac{K_G}{K_G^*}\right)^{\frac{n_G}{n_G-1}} \tag{6}$$

where $C_{E,0}^*$ is the initial pseudo liquid-phase concentration of competing NOM (nmol/L).

The value of n_E, the EBC Freundlich exponent, was unknown. However, the values of q_E^* and $C_{E,0}^*$ defined by Eqs. (1) and (2), respectively, can be used to compare competing-NOM loadings on the carbon particles and to compare initial competing-NOM concentrations if the n_E values are not very different [11,15].

The fact that values of q_E^* were similar for SPAC and PAC for all tested waters (Fig. 2A) clearly indicates that SPAC and PAC adsorbed competing NOM to similar extents at a given carbon dose. However, SPAC adsorbed NOM to a greater extent at a given carbon dose than PAC did, as shown in Fig. 1B. These results suggest that SPAC adsorbed non-competing NOM (NOM that is not competing with geosmin) to a greater extent than PAC did, but that SPAC and PAC adsorbed competing NOM to similar extents. Accordingly, the magnitudes of the effects of NOM on geosmin adsorption were almost the same for SPAC and PAC. The initial concentrations of the

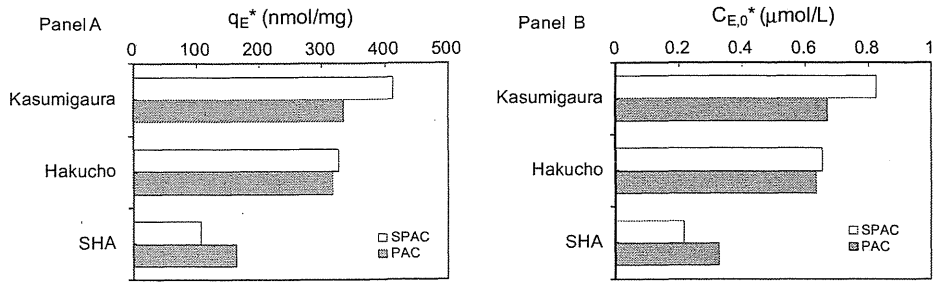

Fig. 2. Panel A: Pseudo solid-phase concentration of geosmin-competing NOM (q_E^*) at a carbon dose of 2 mg/L. Panel B: Initial pseudo liquid-phase concentration of the geosmin-competing NOM ($C_{E,0}^*$).

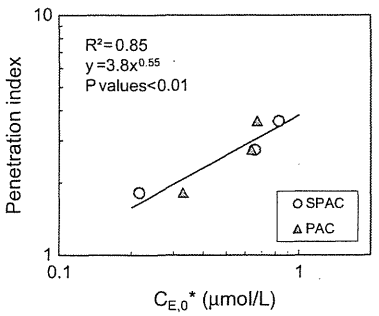

Fig. 3. Relationship between penetration index values and initial pseudo liquid-phase competing-NOM concentrations ($C_{E,0}^*$). The penetration index values were equated to the slope of the logarithm of the median diameter of adsorbent against the logarithm of the DOC solid-phase concentration.

NOM that competes with geosmin ($C_{E,0}^*$) were similar for SPAC and PAC (Fig. 2B).

For MIB adsorption in NOMWs, the values of $C_{E,0}^*$ are highly correlated with the values of the penetration index, which is defined by the slope of plots of the logarithms of the median adsorbent diameters vs. the logarithms of the solid-phase NOM concentrations, and by which the extent of penetration of NOM into carbon particles can be quantitatively evaluated [11,17]. For geosmin in the present study, the correlation obtained was fairly good, as shown in Fig. 3. The positive slope of the correlation plot indicates that the NOM consisted of a high percentage of competing-NOM molecules with a tendency to be highly penetrative. This suggests that the competing NOM penetrated and adsorbed onto interior surfaces of the carbon particles. If so, the extent of competing-NOM loading on SPAC and PAC would be similar. This conclusion is consistent with the results in Fig. 2 and related discussion, in which pseudo solid-phase concentrations, namely, competing-NOM loadings (q_E^*) on SPAC and PAC, were not different.

3.3. Characteristics of NOMs that penetrate and do not penetrate activated carbon

In the previous study of Ando et al. [9], adsorption isotherms on SPAC and PAC were compared for NOM from different sources. These investigators reported that for high-SUVA (specific UV absorbance) NOM the ratio of SPAC to PAC adsorption capacities was high, suggesting that such NOM did not penetrate the carbon particle and preferentially adsorbed near the outer surface of the carbon particle. Instead of this ratio, in the present study we used the reciprocal value of the penetration index, the non-penetration index, to more precisely quantify the degree of limited penetration of NOM from the outer surface to the inner region of carbon particles. We evaluated NOM characteristics by using the data of HPSEC with UV_{260} and DOC detection. We also used NOM adsorption and HPSEC data from previous studies [9,11]. The fact that SUVA values were significantly correlated with non-penetration index values ($R^2 = 0.71$, $P < 0.0001$, Fig. 4A) reflects the tendency of the adsorption capacity to be higher for SPAC than for PAC when the NOM consists mostly of chromophoric NOM. The correlation was much lower but nevertheless significant ($R^2 = 0.28$, $P = 0.028$) between the weight-average MW of the DOC and non-penetration index (Fig. 4B), whereas the correlation was higher and very significant between the weight-average MW of UV_{260} and non-penetration index ($R^2 = 0.75$, $P < 0.0001$, Fig. 4C). These results suggest that MW also plays an important role in the degree of penetration. We then hypothesized that a high-MW fraction of the NOM could penetrate the carbon particle to a lesser extent than a low-MW fraction and would hence preferentially adsorb near the outer surface of activated carbon particles. We calculated the percentages of high-MW NOM fractions in the DOC by integrating partial areas of DOC chromatograms for MWs exceeding certain cutoff levels. We used the product of the SUVA value and the partial area of the UV_{260} chromatograms for MWs exceeding certain cutoff levels as a metric of the chromophoric high-MW fraction. Fig. 5 shows the

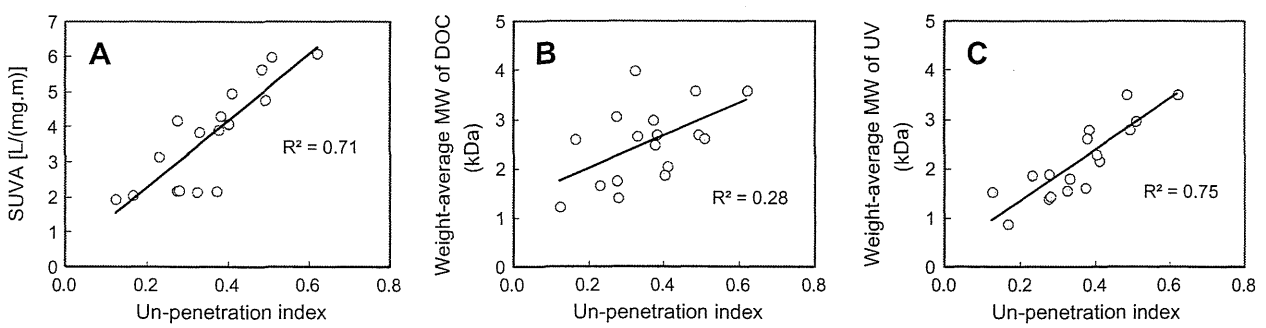

Fig. 4. Plots of un-penetration index values vs. SUVA values (A), weight-average MWs of DOC (B), and weight-average MWs of UV_{260} (C).

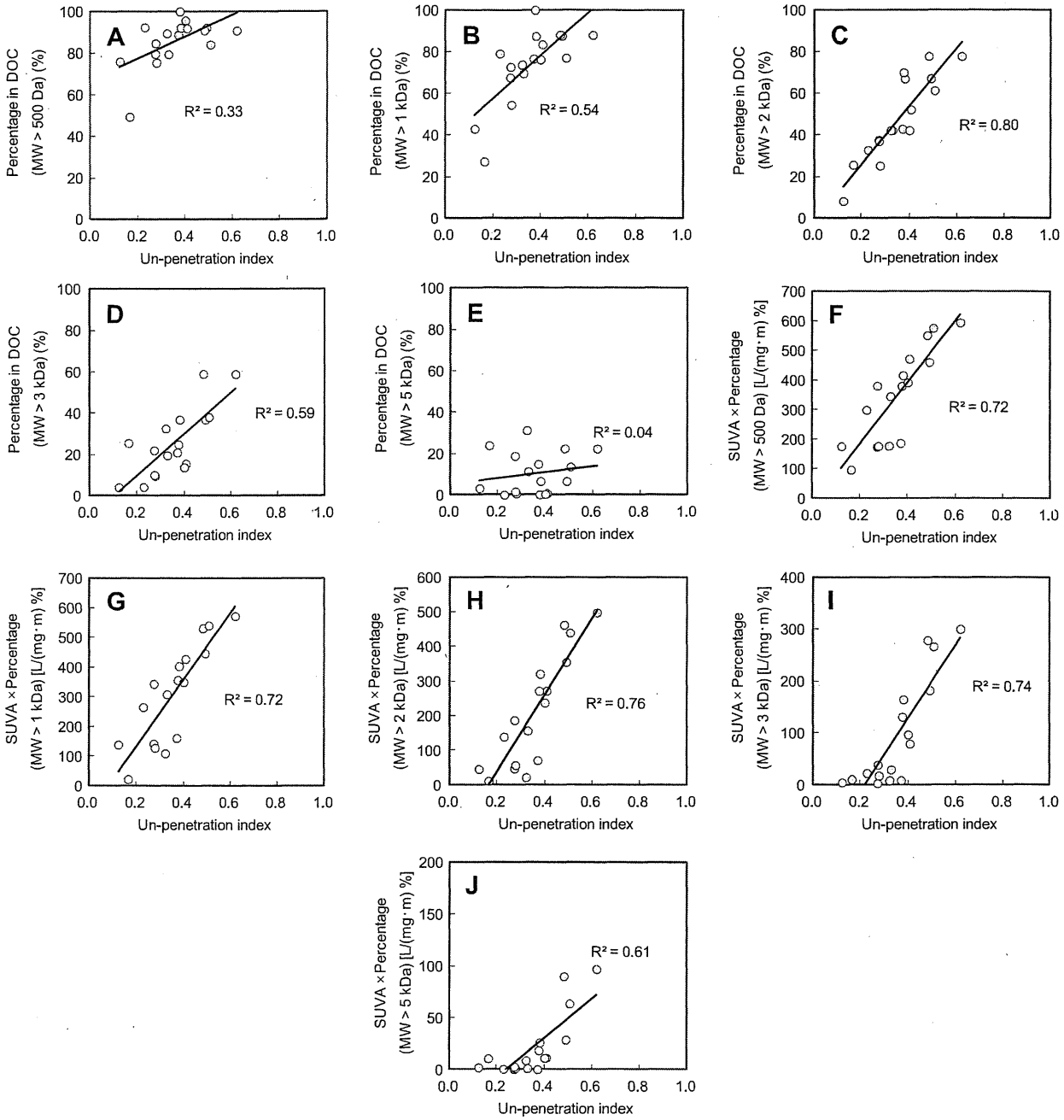

Fig. 5. Plots of un-penetration index values against the fractional areas of DOC chromatograms with MW higher than cutoff levels (Panels A–E) and against the product of SUVA value and fractional areas of UV_{260} chromatogram with MW higher than cutoff levels (Panel F–J).

relationships between the percentages of various high-MW NOM fractions and the non-penetration index values. The correlation was highly significant ($R^2 > 0.7$, $P < 0.0001$) for DOC with MWs of >2 kDa (Fig. 5C) and chromophoric NOM with MWs of >0.5, >1, >2, and > 3 kDa (Fig. 5F–I). Overall, correlations were higher for chromophoric NOM fractions than for DOC fractions (Fig. 6), but a high correlation ($R^2 > 0.75$) was commonly seen for MWs of > 2 kDa for both DOC and chromophoric NOM. It is therefore possible that chromophoric high-MW (MW > 2 kDa) NOM is associated with low penetration into carbon particles. To explore the contrasting characteristics of NOM with high penetrative ability, we plotted low-MW NOM fractional areas, against penetration

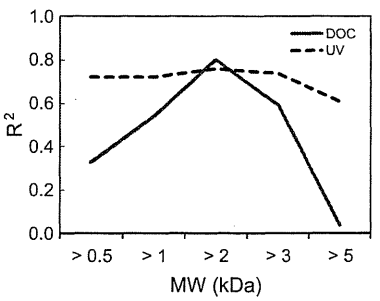

Fig. 6. Change of R^2 for un-penetration index against MW cutoff level.

index values (Fig. 7). A fairly high and significant correlation ($R^2 = 0.69$, $P < 0.0001$) was evident for NOM fractions that consisted of DOC with MWs of <2 kDa (Fig. 7C), but the correlation with chromophoric NOM with MWs of <2 kDa was low and not significant ($P = 0.35$, Fig. 7H, Fig. 8). Therefore nonchromophoric low-MW NOM could probably diffuse into the inner region of carbon particles and adsorb there.

To further confirm these estimates, we divided NOM into four fractions and conducted multiple regression analyses with non-penetration or penetration index values as the dependent variable and the percentages of three NOM fractions out of the total of four fractions as the explanatory (independent) variables. We used a MW of 2 kDa as a cutoff level for the NOM fractionation, on the basis of the results mentioned above in this subsection. The four NOM fractions were (a) chromophoric NOM with MWs of <2 kDa, (b) chromophoric NOM with MWs of >2 kDa, (c) nonchromophoric NOM with MWs of <2 kDa, and (d) nonchromophoric NOM with MWs of >2 kDa (see Table 1). The percentages of the four fractions were calculated from the DOC and UV chromatograms on the basis of the assumption that the SUVA of chromophoric NOM was 6.1 m^{-1} L/mg-C [11,16]. When the non-penetration index was the dependent variable, the explanatory variables were fractions a, b,

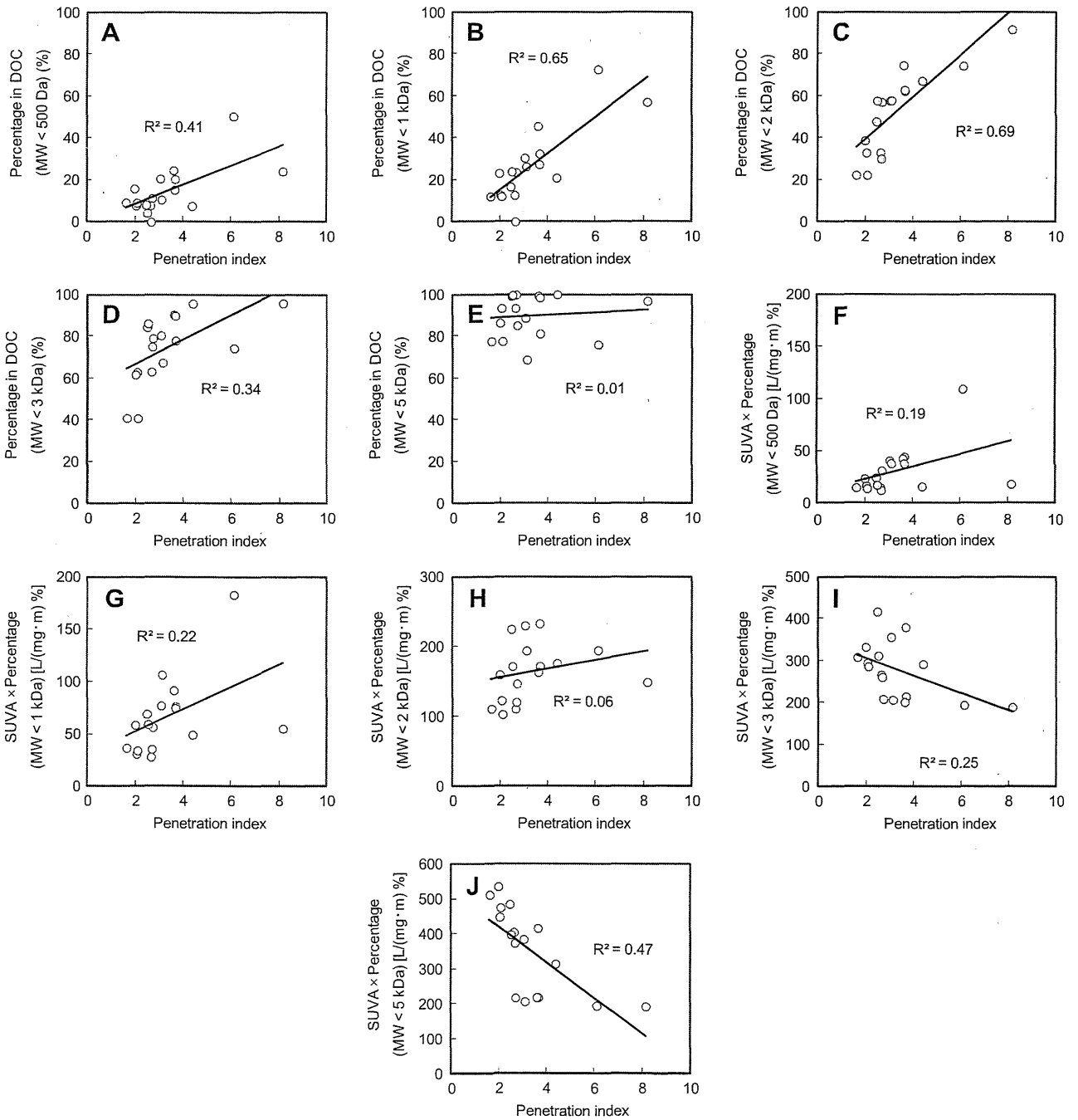

Fig. 7. Plots of penetration index values against the fractional areas of DOC chromatogram with MW lower than cutoff levels (Panels A–E) and against the product of SUVA value and fractional areas of UV_{260} chromatograms with MW lower than cutoff levels (Panels F–J).

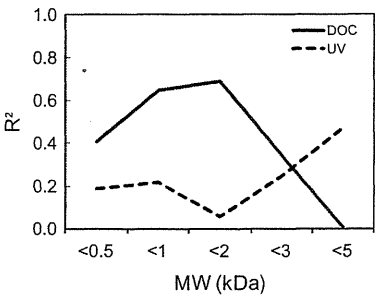

Fig. 8. Change of R^2 for penetration index against MW cutoff level.

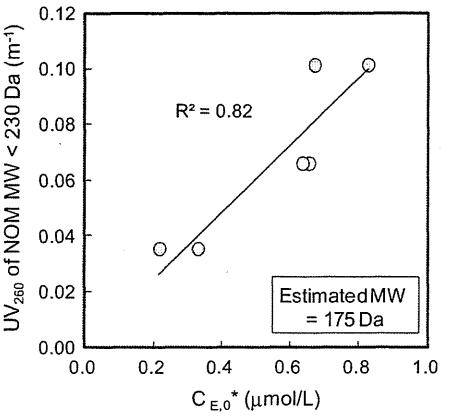

Fig. 9. Relationship between the UV_{260} absorbance of NOM with a MW of <230 Da and the competing-NOM concentration ($C^*_{E,0}$). UV_{260} absorbance values were obtained from size-exclusion chromatograms. $C^*_{E,0}$ values were estimated from geosmin isotherms by using Eq. (2). Coefficients of determination (R^2) were determined from 1 – SSreg/SStot, where SSreg is the sum of squares of the residuals around the regression line with an intercept of 0, and SStot is the sum of squares of the residuals around a horizontal line representing the mean absorbance value of the data shown [18].

and d, fraction c being the most likely to not include non-penetrating NOM. Results are shown in Table 1. Fraction b was associated with a highly significant ($P = 2.2 \times 10^{-5}$) positive regression coefficient. Fraction d was also associated with a significant ($P = 0.028$) positive regression coefficient. It is therefore possible that the NOM that does not penetrate carbon particles and instead adsorbs onto the outer surface of the particles is composed mainly of chromophoric NOM with MWs of >2 kDa. Nonchromophoric NOM with MWs of >2 kDa could also be non-penetrating NOM. When the penetration index was the dependent variable, the explanatory variables were the three fractions a, c, and d, fraction b being the most likely to not include penetrating NOM. The fact that fraction c was associated with a positive and highly significant ($P = 2.8 \times 10^{-5}$) regression coefficient indicates that the penetrating NOM was composed mainly of nonchromophoric NOM with MWs of <2 kDa.

3.4. Characteristics of NOMs that compete and do not compete with geosmin

The previous study [11] revealed that MIB competes with very-low-MW (MW < 230 Da) chromophoric NOM. We assumed the NOM that competes with geosmin to be similar to that of MIB because the MW of geosmin (182 Da) is similar to that of MIB (168 Da). We plotted the UV_{260} absorbance of very-low-MW NOM, which we obtained from the fraction of the area of the UV_{260} chromatogram with MW of <230 Da, against the initial concentration of the NOM that competes with geosmin (Fig. 9). The slope of the linear relationship is the ratio of UV_{260} to $C^*_{E,0}$. The ratio is theoretically given by

$$\frac{UV_{260}}{C^*_{E,0}} = \frac{SUVA \times Cabon\ content \times MW}{n_E^{\frac{n_M}{n_M-1}}} \quad (7)$$

If the NOM that competes with geosmin is a chromophoric NOM, as is the case with MIB, its MW can be estimated by using Eq. (7). The estimated MW was 175 Da if we assumed the SUVA value and carbon content of the chromophoric NOM in Eq. (7) to be 6.12 cm^{-1} L/mg and 52%, respectively (International Humic Substances Society, 2012; [11,16]). The estimated MW of 175 Da corroborated the cutoff MW value of 230 Da. When the cutoff MW values were changed, the estimated MWs changed accordingly, as shown in Table 2. The cutoff MW and the estimated MW were in agreement only when the cutoff MW was 230 Da. When DOC concentrations were used instead of UV_{260} absorbances and the DOC MW fractions were plotted against $C^*_{E,0}$, none of the plots produced agreement between the cutoff and estimated MWs (Table 2). The estimated MW (175 Da) of competing NOM is very close to the MW of geosmin (182 Da). Moreover the R^2 value is also high. The result therefore confirms that the competing NOM has a molecular size similar to that of the targeted micro-pollutant, a conclusion suggested from the MIB experiments [11]. If the MW of the competing NOM is 175 Da, the concentration of competing NOM in the NOM waters accounts for <2% of the total DOC concentration.

Section 3.4 has revealed that the competing NOM consists of very-low-MW (<230 Da) chromophoric NOM, whereas Section 3.2 revealed the competing NOM to be a penetrating-NOM. Therefore, the very-low-MW (<230 Da) chromophoric NOM appears to be a penetrating NOM, though penetrating NOM is composed mainly of low-MW nonchromophoric NOM (Section 3.3). The low-MW nonchromophoric NOM would probably not compete with geosmin, although it diffuses into the inner region and adsorb to internal adsorption sites. Such NOM, because of its molecular size, would not mostly have access to pores where geosmin adsorbs. We also suspect that the adsorption affinity of such NOMs to

Table 1
Regression analyses for NOM that penetrates and does not penetrate activated carbon.

Designation		Fraction a	Fraction b	Fraction c	Fraction d
Dependent variable = un-penetration index value	R^2	Chromophoric NOM MW < 2 kDa	MW > 2 kDa	Nonchromophoric NOM MW < 2 kDa	MW > 2 kDa
		Fraction a	Fraction b	Fraction c	Fraction d
Coefficient	0.83	0.0014	0.0057		0.0038
P-value		0.60	2.2×10^{-5}		0.028
Dependent variable = penetration index value	R^2	Chromophoric NOM MW < 2 kDa	MW > 2 kDa	Nonchromophoric NOM MW < 2 kDa	MW > 2 kDa
Coefficient	0.77	0.077		0.085	−0.01
P-value		0.82		2.8×10^{-5}	0.56

Table 2
MW estimated from the slope of the plot of the concentration of the low-MW fraction and competing-NOM concentration, and the coefficients of determination (R^2) of the plots. Coefficients of determination were equated to 1 – SSreg/SStot, where SSreg is the sum of squares of the residuals around the regression line with an intercept of 0, and SStot is the sum of squares of the residuals around a horizontal line representing the mean absorbance value of the data shown [18].

	Cutoff MW (Da)	<1000	<500	<300	<250	<230	<200
UV_{260}	Estimated MW from the slope (Da)	2130	1150	433	263	175	13
	R^2	0.68	0.92	0.73	0.57	0.82	0.29
DOC	Estimated MW from the slope (Da)	5280	3480	2700	2030	1600	1060
	R^2	0.88	0.76	−0.2	−0.41	−4.6	−4.2

activated carbon is weak and hence that they would not compete effectively with a strong adsorbate such as geosmin.

4. Conclusions

NOM with a high-MW (>2 kDa) and with a chromophoric moiety adsorbs onto the external surface of activated carbon particles. Therefore, when NOM consists mostly of such NOM, SPAC adsorbs NOM to a greater extent than does PAC. Contrariwise, low-MW (<2 kDa) nonchromophoric NOM can adsorb to internal adsorption sites in carbon particles. Therefore, SPAC and PAC adsorb low-MW NOM to a similar extent.

NOM that competes with geosmin for adsorption is a very-low-MW (<230 Da) chromophoric NOM, as is the NOM that competes with another micro-pollutant, MIB. The NOM fraction that competes with a target compound for adsorption has a molecular weight similar to that of the target compound. We estimate that the competing NOM accounts for <2% of the total DOC.

- The competing NOM can also adsorb onto internal adsorption sites in carbon particles. Although there is higher NOM loading onto SPAC than PAC, the NOM effect on micro-pollutant adsorption capacity is no more severe for SPAC than for PAC, because SPAC and PAC adsorb the competing NOM, which accounts for only a small fraction of the entire NOM, to a similar extent

Acknowledgements

This study was supported by Grant-in-Aid for Scientific Research A(21246083), S(24226012) and Challenging Exploratory Research (23656323) from the Japan Society for the Promotion of Science, by Health and Labour Sciences Research Grant (Research on Health Security Control) of Japan, and by Metawater Co., Tokyo, Japan.

Appendix A. Supplementary material

Supplementary data associated with this article can be found, in the online version, at http://dx.doi.org/10.1016/j.seppur.2013.04.009.

References

[1] W.F. Young, H. Horth, R. Crane, T. Ogden, M. Arnott, Taste and odour threshold concentrations of potential potable water contaminants, Water Res. 30 (2) (1996) 331–340.
[2] J.L. Worley, A.M. Dietrich, R.C. Hoehn, Dechlorination techniques to improve sensory odor testing of geosmin and 2-MIB, J. Am. Water Works Assoc. 95 (3) (2003) 109–117.
[3] R. Srinivasan, G.A. Sorial, Treatment of taste and odor causing compounds 2-methyl isoborneol and geosmin in drinking water: a critical review, J. Environ. Sci. 23 (1) (2011) 1–13.
[4] H. Sontheimer, J.C. Crittenden, R.S. Summers, Activated Carbon for Water Treatment, second ed., DVGW-Forschungsstelle, Karlsruhe, Germany, 1988.
[5] Y. Matsui, Y. Fukuda, R. Murase, N. Aoki, S. Mima, T. Inoue, T. Matsushita, Micro-ground powdered activated carbon for effective removal of natural organic matter during water treatment, Water Sci. Technol.: Water Supply 4 (4) (2004) 155–163.
[6] Y. Matsui, R. Murase, T. Sanogawa, H. Aoki, S. Mima, T. Inoue, T. Matsushita, Rapid adsorption pretreatment with submicrometre powdered activated carbon particles before microfiltration, Water Sci. Technol. 51 (6–7) (2005) 249–256.
[7] Y. Matsui, T. Aizawa, F. Kanda, N. Nigorikawa, S. Mima, Y. Kawase, Adsorptive removal of geosmin by ceramic membrane filtration with super-powdered activated carbon, J. Water Supply Res. Technol.-AQUA 56 (6–7) (2007) 411–418.
[8] Y. Matsui, N. Ando, H. Sasaki, T. Matsushita, K. Ohno, Branched pore kinetic model analysis of geosmin adsorption on super-powdered activated carbon, Water Res. 43 (12) (2009) 3095–3103.
[9] N. Ando, Y. Matsui, R. Kurotobi, Y. Nakano, T. Matsushita, K. Ohno, Comparison of natural organic matter adsorption capacities of super-powdered activated carbon and powdered activated carbon, Water Res. 44 (14) (2010) 4127–4136.
[10] Y. Matsui, Y. Nakano, N. Ando, H. Sasaki, K. Ohno, T. Matsushita, Geosmin and 2-methylisoborneol adsorption on super-powdered activated carbon in the presence of natural organic matter, Water Sci. Technol. 62 (11) (2010) 2664–2668.
[11] Y. Matsui, T. Yoshida, S. Nakao, D.R.U. Knappe, T. Matsushita, Characteristics of competitive adsorption between 2-methylisoborneol and natural organic matter on superfine and conventionally sized powdered activated carbons, Water Res. 46 (15) (2012) 4741–4749.
[12] M.R. Graham, R.S. Summers, M.R. Simpson, B.W. MacLeod, Modeling equilibrium adsorption of 2-methylisoborneol and geosmin in natural waters, Water Res. 34 (8) (2000) 2291–2300.
[13] D.R.U. Knappe, Y. Matsui, V.L. Snoeyink, P. Roche, M.J. Prados, M.M. Bourbigot, Predicting the capacity of powdered activated carbon for trace organic compounds in natural waters, Environ. Sci. Technol. 32 (11) (1998) 1694–1698.
[14] S. Qi, L. Schideman, B.J. Mariñas, V.L. Snoeyink, C. Campos, Simplification of the IAST for activated carbon adsorption of trace organic compounds from natural water, Water Res. 41 (2) (2007) 440–448.
[15] G. Newcombe, J. Morrison, C. Hepplewhite, D.R.U. Knappe, Simultaneous adsorption of MIB and NOM onto activated carbon – II. competitive effects, Carbon 40 (12) (2002) 2147–2156.
[16] International Humic Substance Society, <http://www.ihss.gatech.edu/soilhafa.html>, (accessed 23.04.12).
[17] Y. Matsui, N. Ando, T. Yoshida, R. Kurotobi, T. Matsushita, K. Ohno, Modeling high adsorption capacity and kinetics of organic macromolecules on super-powdered activated carbon, Water Res. 45 (4) (2011) 1720–1728.
[18] H.J. Motulsky, A. Christopoulos, Fitting Models to Biological Data Using Linear and Nonlinear Regression: A Practical Guide to Curve Fitting, Oxford University Press, New York, 2004.